

1. Report No. FHWA/TX-87+437-1		2. Government Accession No.		3. Recipient's Catalog No.	
4. Title and Subtitle DYNAMIC INTERPRETATION OF DYNAFLECT AND FALLING WEIGHT DEFLECTOMETER TESTS ON PAVEMENT SYSTEMS				5. Report Date August 1986	
				6. Performing Organization Code	
7. Author(s) Ko-Young Shao, J. M. Roesset, and K. H. Stokoe, II				8. Performing Organization Report No. Research Report 437-1	
9. Performing Organization Name and Address Center for Transportation Research The University of Texas at Austin Austin, Texas 78712-1075				10. Work Unit No.	
				11. Contract or Grant No. Research Study 3-8-85-437	
12. Sponsoring Agency Name and Address Texas State Department of Highways and Public Transportation; Transportation Planning Division P. O. Box 5051 Austin, Texas 78763-5051				13. Type of Report and Period Covered Interim	
				14. Sponsoring Agency Code	
15. Supplementary Notes Study conducted in cooperation with the U. S. Department of Transportation, Federal Highway Administration. Research Study Title: "Utilization of Surface Wave System for Measuring Moduli of Pavements"					
16. Abstract The Dynaflect and the Falling Weight Deflectometer are commonly used for non-destructive testing of pavements. Although in both cases a dynamic load is imparted, the determination of the mechanical properties of the pavement is normally performed by using static analyses. In this study, the displacements obtained from dynamic analyses are compared to those provided by conventional static programs when the sub-base is a homogeneous soil stratum of finite depth, resting on a much stiffer rock-like material and when the soil properties increase smoothly with depth, as is often the case. The results of these comparisons indicate that for certain ranges of depth to bedrock a static interpretation of the Dynaflect and Falling Weight Deflectometer tests may lead to substantial errors. Situations where these errors are important are more likely to be encountered with the Dynaflect than with the Falling Weight Deflectometer.					
17. Key Words pavements, deflections, Dynaflect, Falling Weight Deflectometer, non-destructive testing, seismic waves			18. Distribution Statement No restrictions. This document is available to the public through the National Technical Information Service, Springfield, Virginia 22161.		
19. Security Classif. (of this report) Unclassified		20. Security Classif. (of this page) Unclassified		21. No. of Pages 78	22. Price

**DYNAMIC INTERPRETATION OF DYNAFLECT AND FALLING WEIGHT
DEFLECTOMETER TESTS ON PAVEMENT SYSTEMS**

by

Ko-Young Shao
J. M. Roesset
K. H. Stokoe, II

Research Report Number 437-1

Utilization of Surface Wave System for
Measuring Moduli of Pavements
Research Project 3-8-85-437

conducted for

Texas State Department of Highways
and Public Transportation

in cooperation with the
U.S. Department of Transportation
Federal Highway Administration

by the

CENTER FOR TRANSPORTATION RESEARCH
BUREAU OF ENGINEERING RESEARCH
THE UNIVERSITY OF TEXAS AT AUSTIN

August 1986

The contents of this report reflect the views of the authors, who are responsible for the facts and the accuracy of the data presented herein. The contents do not necessarily reflect the official views or policies of the Federal Highway Administration. This report does not constitute a standard, specification, or regulation.

PREFACE

This report describes work done on the project entitled "Utilization of Surface Wave System for Measuring Moduli of Pavements." This project is being conducted at the Center for Transportation Research, The University of Texas at Austin, as part of the Cooperative Highway Research Program sponsored by the State Department of Highways and Public Transportation and the Federal Highway Administration.

This report presents the results of analytical studies to evaluate the importance of dynamic effects on the deflections measured in the Dynaflect and Falling Weight Deflectometer tests. From the results of these studies it is concluded that dynamic effects may be important when there is bedrock at a finite depth. In this case a formulation which accounts for the dynamic nature of the loading should be used.

The writers are particularly grateful to the entire staff of the Center for Transportation Research, who provided support throughout the analysis and preparation stages of this report.

Ko-Young Shao
J.M. Roesset
K.H. Stokoe

LIST OF REPORTS

Report No. 437-1, "Dynamic Interpretation of Dynaflect and Falling Weight Deflectometer Tests on Pavement Systems," by Ko-Young Shao, J.M. Roesset, and K.H. Stokoe, II, presents the results of analytical studies of the dynamic effects of Dynaflect and Falling Weight Deflectometer tests, based on the consideration of wave propagation including body waves (p and s waves) and Rayleigh waves.

ABSTRACT

The Dynaflect and the Falling Weight Deflectometer are commonly used for nondestructive testing of pavements. Although in both cases a dynamic load is imparted, the determination of the mechanical properties of the pavement is normally performed by using static analyses. In this study, the displacements obtained from dynamic analyses are compared to those provided by conventional static programs when the sub-base is a homogeneous soil stratum of finite depth, resting on a much stiffer rock-like material and when the soil properties increase smoothly with depth, as is often the case. The results of these comparisons indicate that for certain ranges of depth to bedrock a static interpretation of the Dynaflect and Falling Weight Deflectometer tests may lead to substantial errors. Situations where these errors are important are more likely to be encountered with the Dynaflect than with the Falling Weight Deflectometer.

KEY WORDS: pavements, deflections, Dynaflect, Falling Weight Deflectometer, nondestructive testing, seismic waves

SUMMARY

The Dynaflect and the Falling Weight Deflectometer are commonly used for nondestructive testing of pavements. Although in both cases a dynamic load is applied, the determination of the mechanical properties of the pavement, base and subgrade is normally performed comparing the measured deflections at various points along the surface to results of static analyses considering the subgrade as a homogeneous, elastic half space. In this report a more accurate model to compute the displacements along the surface of a pavement due to a dynamic load is presented. The formulation starts by considering steady state harmonic forces and displacements. For a harmonic excitation at a fixed frequency (case of the Dynaflect) the solution provides directly the desired results. For an arbitrary transient excitation (case of the Falling Weight Deflectometer) the time history of the specified forces must be decomposed into different frequency components using a Fourier Transform. Results are obtained then for each frequency and combined to obtain the time history of displacements through the Inverse Fourier Transform.

Deflections obtained from the dynamic analyses are compared to those provided by conventional static programs when the subgrade is a homogeneous soil stratum of finite depth, resting on a much stiffer, rock-like, material and when the soil properties increase smoothly with depth, as is often the case. The results of these comparisons show that for certain ranges of depth to bedrock a static interpretation of the Dynaflect and Falling Weight Deflectometer tests may lead to substantial errors. Situations where these errors are important are more likely to be encountered with the Dynaflect than with the Falling Weight Deflectometer.

IMPLEMENTATION STATEMENT

The Dynaflect and the Falling Weight Deflectometer are the instruments most commonly used by the Texas State Department of Highways and Public Transportation to obtain data concerning the in situ properties of pavements. The elastic properties of the pavement, base and subgrade are normally backfigured by comparing the deflections measured at various points along the surface to the results of static analyses assuming a homogeneous elastic half-space for the subgrade. The studies described in this report were conducted in order to assess the potential errors associated with the use of static analyses to backfigure the pavement, base and subgrade moduli from the deflection basin caused by a dynamic load. The results seem to indicate that these errors, due to dynamic effects, can be important when the subgrade has a finite thickness and is underlain by much stiffer, rock-like material. They are likely to be more significant for the Dynaflect than for the Falling Weight Deflectometer.

Since these studies are only of a theoretical nature further parametric studies and experimental verification are needed before more definite recommendations can be made. If one were to find, however, strange or unusual results with the use of the present approach, it may be advisable to determine whether there is rock at a shallow depth. In this case dynamic effects could provide an explanation for the anomaly in the results, particularly if the frequency of the excitation is in the range between the fundamental frequencies of the stratum in shear and dilatation.

TABLE OF CONTENTS

	Page
PREFACE.....	iii
LIST OF REPORTS.....	v
ABSTRACT.....	vii
SUMMARY.....	ix
IMPLEMENTATION STATEMENT.....	xi
LIST OF TABLES.....	xv
LIST OF FIGURES.....	xvii
CHAPTER 1. INTRODUCTION.....	1
1.1 Existing Testing Methods.....	1
1.2 New Procedure.....	1
1.3 Purpose of Study.....	2
CHAPTER 2. FORMULATION.....	3
2.1 Introduction.....	3
2.2 Wave Equation in Cartesian Coordinate.....	5
2.3 Plane Waves.....	9
2.4 Wave Equations in Cylindrical Coordinate.....	10
2.5 Discrete Model.....	12
CHAPTER 3. SIMULATION OF DYNAFLECT TESTS.....	17
3.1 Introduction.....	17
3.2 Application to a Pavement System.....	17
3.3 Estimation of Material Properties.....	32
CHAPTER 4. SIMULATION OF FALLING WEIGHT DEFLECTOMETER TESTS.....	35
4.1 Introduction.....	35
4.2 Determination of Transient Response.....	35
4.3 Estimation of Material Properties.....	42
CHAPTER 5. CONCLUSIONS AND RECOMMENDATIONS.....	57
BIBLIOGRAPHY.....	59

LIST OF TABLES

Table		Page
3.1	Deflection Bulbs and Predicted Elastic Moduli for Homogeneous Sub-Base and Different Depths to Bedrock.....	33
4.1	Deflection Bulbs and Predicted Elastic Moduli for Homogeneous Sub-Base and Different Depths to Bedrock. Falling Weight Deflectometer.....	55

LIST OF FIGURES

Figure	Page
3.1 Geometric Configuration of Loads and Stations for Dynaflect.....	18
3.2 Profile of Pavement Used for Studies.....	19
3.3 Variation of Static Displacements with Depth to Bedrock - Dynaflect.....	20
3.4 Variation of Dynamic Displacements with Depth to Bedrock - Dynaflect.....	21
3.5 Ratio of Dynamic to Static Displacements, Points 1 and 5 - Dynaflect.....	23
3.6 Ratio of Dynamic to Static ($H = \infty$) Displacements, Points 1 and 5 - Dynaflect.....	24
3.7 Variation of Dynamic Displacements with Depth to Bedrock - Dynaflect, $D = 0.02$	25
3.8 Ratio of Dynamic to Static Displacements, Points 1 and 5, $D = 0.02$	26
3.9 Ratio of Dynamic to Static ($H = \infty$) Displacements, Points 1 and 5 - Dynaflect, $D = 0.02$	27
3.10 Variation of Static Displacements with Depth to Bedrock - Dynaflect, G Inc.	28
3.11 Variation of Dynamic Displacements with Depth to Bedrock - Dynaflect, G Inc.	29
3.12 Ratio of Dynamic to Static Displacements, Points 1 and 5, G Inc.	30
3.13 Ratio of Dynamic to Static ($H = \infty$) Displacements for Variable Soil Profile - Dynaflect.....	31
4.1 Geometric Configuration of Loads and Stations for Dynaflect and Falling Weight Deflectometer.....	36
4.2 Time History of Impulse Load.....	37
4.3 Amplitude Spectrum of Linear Impulse Load.....	38

Figure	Page
4.4 Transfer Function at Point 1 (Center of Load) H = 20 ft - Falling Weight Deflectometer.....	39
4.5 Profile of Pavement Used for Studies.....	40
4.6 Time History of Displacements at Points 1 and 7, H = 20 ft.....	43
4.7 Displacement Bowls of 1. Static, 2. Dynamic, H = 20 ft.....	44
4.8 Ratio of Dynamic (Imp.) to Static and Static (H = ∞) Displacements, H = 20 ft - Falling Weight Deflectometer.....	45
4.9 Transfer Function at Point 1 (Center of Load), H = 40 ft - Falling Weight Deflectometer.....	46
4.10 Response Time History of Displacements at Points 1 and 7, H = 40 ft - Falling Weight Deflectometer.....	47
4.11 Displacement Bowls of 1. Static, 2. Dynamic, H = 40 ft.....	48
4.12 Ratio of Dynamic to Static and Static (H = ∞) Displacements, H = 40 ft - Falling Weight Deflectometer.....	49
4.13 Transfer Function at Point 1 (Center of Load), H = 80 ft - Falling Weight Deflectometer.....	50
4.14 Response Time History of Displacements at Points 1 and 7, H = 80 ft, Falling Weight Deflectometer.....	51
4.15 Displacement Bowls of 1. Static, 2. Dynamic, H = 80 ft.....	52
4.16 Ratio of Dynamic to Static and Static (H = ∞) Displacements, H = 80 ft - Falling Weight Deflectometer.....	53

CHAPTER 1. INTRODUCTION

1.1 Existing Test Methods

A number of methods have been proposed to evaluate the elastic properties of pavement systems. Some of them, like the plate bearing test, the curvature meter, the Benkelman beam, the traveling deflectometer and the La Croix deflectograph are based on the application of static loads and measurement of the corresponding pavement deflections. Elastic layer theory is then used to backfigure, from the measured deflections, the pavement, base and sub-base moduli. Others are based on the application of dynamic loads, either at a fixed frequency (steady state vibrations), or in the form of an impact. The Dynaflect, the Road Rater and the WES and FHWA Vibrators belong to the first group, while the Falling Weight Deflectometer belongs to the second. Although these tests are dynamic by nature, the interpretation of their results to estimate the elastic properties of the pavement, base and sub-base relies on static analyses. These analyses assume furthermore that the soil in the sub-base is an elastic, homogeneous and isotropic half-space. In most cases soil properties will vary with depth and the soil will be underlain at some depth by stiffer, rock-like material.

1.2 New Procedure

A new procedure that seems to be very promising is the Spectral Analysis of Surface Waves (SASW) method, which is being developed at The University of Texas at Austin. In this method a transient impact is applied on the surface of the pavement and the deflections are recorded at two target points with the help of a Spectral Analyzer. The time histories of the deflections are automatically decomposed into a large number of frequency components and the apparent velocity of propagation of the waves between the two target points is determined at each frequency. Waves with high frequencies (short wave lengths) will penetrate only a small distance from the surface and their velocity of propagation should reflect the material properties of a top layer with a thickness of the order of the wavelength. Waves with low frequencies reflect on the other hand average material properties over a large depth. It is thus possible, starting with the high frequency components and proceeding with

smaller frequencies, to determine the moduli of the pavement, base and subgrade at different depths. Interpretation of the results of the SASW method is performed at present assuming that only surface (Rayleigh) waves are generated by the impact. Since near the source P and S waves (body waves) are also important the distance between the first receiver and the source must be large enough to guarantee that a sufficient amount of body wave energy has dissipated. On the other hand if the source is too far from the first receiver, or the distance between the two receivers is large in relation to the wavelengths involved, the amplitude of the arriving waves may be too small and background noise may dominate the records.

1.3 Purpose of Study

The purpose of this work was to develop a more accurate mathematical model to study the propagation of waves generated by a surface impact through a pavement system, accounting not only for surface (Rayleigh) waves, but also for the presence of body waves. A number of formulations were explored and the one presented by Kausel (13) was selected. A review of these formulations is presented in Chapter 2. A computer program was implemented using Kausel's formulation and parametric studies were conducted to assess the accuracy of the results. The computer program was then used to evaluate the dynamic effects present in the results obtained with the Dynaflect (Chapter 3) and the Falling Weight Deflectometer (Chapter 4). For this purpose the dynamic displacements computed with the program for various depths to bedrock (thickness of the subgrade) were compared with those resulting from static analyses for the same soil profile, and assuming that the subgrade extends to infinity with uniform properties (the normal assumption in the interpretation of the Dynaflect or Falling Weight Deflectometer results). The dynamic deflection bulbs obtained from the analyses were also used as input for the standard backfiguring process (Ref 24) to estimate the elastic moduli of the pavement, base and sub-base, in order to assess the errors induced by neglecting dynamic effects.

CHAPTER 2. FORMULATION

2.1 Introduction

Consider a soil deposit consisting of horizontal layers. The mass density and elastic moduli of the soil may change with depth, from layer to layer, but are assumed to be constant over each layer. For the present application the top layer would represent the pavement (assuming that it extends to infinity in both horizontal directions), the second layer would be the base, and the remaining layers represent the soil of the sub-base. The determination of the response of this soil deposit to dynamic loads applied at the surface (or at any point within the soil mass) falls mathematically into the area of wave propagation theory.

The formulation of these problems always starts by considering steady state harmonic forces and displacements at a given frequency. For a harmonic excitation, as caused by a vibrating machine rotating at a specified velocity (case of the Dynaflect) the solution at the corresponding frequency provides directly the desired results. For an arbitrary transient excitation (case of the Falling Weight Deflectometer) the time history of the specified forces must be decomposed into different frequency components using a Fourier series, or more conveniently a Fourier transform. Results are obtained then for each term of the series (each frequency) and combined to obtain the time history of displacements (Inverse Fourier transform).

Considering an isolated layer with uniform properties the stresses and displacements along the top and bottom surfaces can be expanded in a double Fourier series (or Fourier transform) in the two horizontal directions for cartesian coordinates or in a Fourier series in the circumferential direction and a series of modified Bessel functions in the radial direction for cylindrical coordinates. For each term of these series, corresponding to a given wave number, one can determine closed form analytical expressions in the form of a transfer matrix relating amplitudes of stresses and displacements at the bottom surface to the corresponding quantities at the top (or vice versa). This approach is due to Thomson (23) and Haskell (8) and has served as the basis for most studies on wave propagation through layered media in the last 30 years. An alternative is to relate the stresses at both surfaces to the displacements,

obtaining a dynamic stiffness matrix for the layer [Kausel and Roesset (14)] which can be used and understood in much the same way as those in structural analysis. For a half-space the stiffness matrix relates directly stresses and displacements at the top surface, since the bottom surface is pushed to infinity. Assembling the stiffness matrices of the different layers one can obtain a stiffness matrix for the complete soil deposit relating forces per unit of area applied at the free surface, or the interfaces between the layers, to the displacements at the same elevations.

The terms of the transfer or stiffness matrices of each layer are transcendental functions (complex exponentials). In addition results must be obtained for each term of the Fourier series decomposition (each wave number), then combined, normally by numerical integration, to obtain the solution for a specified load distribution. On the other hand, the thickness of the layers is controlled only by physical considerations and the assumption of uniform properties. This makes the procedure particularly convenient when dealing with a homogeneous half-space or a very small number of layers, but extremely expensive when a large number of layers is needed to reproduce properly the variation of soil properties with depth. Formulations along these lines have been implemented by Gazetas (7) in cartesian coordinates, and by Apsel (3) in cylindrical coordinates.

When the layers are very thin, on the other hand, the transcendental functions representing the variation of displacements with depth can be approximated over each layer by a straight line (or higher order polynomial expansions). The solution (displacements and stresses) is then expressed in terms of the exact analytical expressions in the two horizontal (or radial and circumferential) directions, and in terms of simpler polynomial expansions in the vertical direction (as in a finite element formulation). This approximation leads to much simpler algebraic expressions for the terms of the transfer or stiffness matrices of the layers. In addition, when the soil is underlain by a much stiffer, rock-like material, which can be considered rigid, one can determine the wave numbers (eigenvalues) and the mode shapes (eigenvectors) of the waves propagating through the soil deposit by solving an algebraic eigenvalue problem [Waas (25), Kausel (12)]. Expressing the solution in terms of these mode shapes (eigen-function expansion) Kausel (13) was able to obtain explicit solutions for the displacements caused by harmonic dynamic loads in a layered soil deposit. Kausel's formulation is particularly efficient from the point of view of computation but the layers must be sufficiently thin to re-

produce accurately the variation of the displacements with depth with a piecewise linear approximation. This may require a large number of layers when dealing with a deep soil deposit.

2.2 Wave Equation in Cartesian Coordinates

The wave equations for a harmonic steady state motion in cartesian coordinates can be expressed as:

$$\nabla^2 \varepsilon = (-\omega^2/C_p^2) (\partial^2 \varepsilon / \partial t^2)$$

$$\nabla^2 \Omega = (-\omega^2/C_s^2) (\partial^2 \Omega / \partial t^2)$$

where ε is the volumetric strain $\varepsilon = \text{Div } u = \partial u / \partial x + \partial v / \partial y + \partial w / \partial z$ and Ω is the rotation vector.

$$\Omega_x = 1/2 [(\partial w / \partial y) - (\partial v / \partial z)]$$

$$\Omega_y = 1/2 [(\partial u / \partial z) - (\partial w / \partial x)]$$

$$\Omega_z = 1/2 [(\partial v / \partial x) - (\partial u / \partial y)]$$

$C_p = \sqrt{(\lambda + 2G)/\rho}$ is the compressional (p) wave velocity of the material

$C_s = \sqrt{G/\rho}$ is the shear (s) wave velocity

G is the shear modulus, $\lambda + 2G$ the constrained modulus and ρ the mass density.

In terms of Young's modulus E and Poisson's ratio ν

$$\lambda = \nu E / [(1+\nu)(1-2\nu)] \quad , \quad G = E / [2(1+\nu)]$$

$$\lambda + 2G = E(1-\nu) / [(1-2\nu)(1+\nu)]$$

A general solution of the wave equations can be expressed as a combination of terms of the form

$$U_p = \begin{Bmatrix} u \\ v \\ w \end{Bmatrix}_p = \begin{Bmatrix} l \\ m \\ n \end{Bmatrix} A_p f_p$$

and

$$U_s = \begin{Bmatrix} u \\ v \\ w \end{Bmatrix}_s = \frac{1}{\sqrt{l'^2 + m'^2}} \begin{Bmatrix} -m' & -l'n' \\ l' & -m'n' \\ 0 & l'^2 + m'^2 \end{Bmatrix} \begin{Bmatrix} A_{SH} \\ A_{SV} \end{Bmatrix} f_s$$

with

$$\begin{aligned} l^2 + m^2 + n^2 &= 1 \\ l'^2 + m'^2 + n'^2 &= 1 \end{aligned}$$

A_p represents the amplitude of compressional (p) waves and A_{SH} A_{SV} the amplitudes of shear (SH and SV) waves

$$f_p = \exp[i (\omega/C_p) (-lx - my - nz)]$$

$$f_s = \exp[i (\omega/C_s) (-l'x - m'y - n'z)]$$

When the coefficients l, m, n, l', m', n' , are all real they represent the direction cosines of the direction of propagation of the P and S waves respectively (body waves). When some of them are complex the expressions represent generalized surface waves.

For a horizontally layered soil deposit, considering a layer with homogeneous, isotropic properties one can impose the condition

$$\omega l/C_p = \omega l'/C_s = \xi$$

$$\omega m/C_p = \omega m'/C_s = \eta$$

to have a unique variation of the motions in the x and y directions. ξ and η are the wave numbers and ω/ξ , ω/η are the apparent wave velocities (phase velocities) in the x and y directions. It is then possible to express the general solution as a combination of terms of the form

$$U = \begin{pmatrix} u \\ v \\ iw \end{pmatrix} = \begin{pmatrix} p & -q & sp & p & -q & -sp \\ q & p & sq & q & p & -sq \\ r & 0 & 1 & -r & 0 & 1 \end{pmatrix} E_z A f = C E_z A f$$

$$E_z = \text{diag} \{e^{-krz}, e^{-ksz}, e^{-ksz}, e^{krz}, e^{ksz}, e^{ksz}\}$$

$$A = \sqrt{\ell'^2 + m'^2} \left\{ \frac{1}{\alpha} A_p', A_{SH}'/\sqrt{\ell'^2 + m'^2}, iA_{SV}' \right. \\ \left. (1/\alpha)A_p'', A_{SH}''/\sqrt{\ell'^2 + m'^2}, iA_{SV}'' \right\}^T$$

where

$$f = \exp i(-\xi x - \eta y) \\ k = (\omega/C_s) \sqrt{\ell'^2 + m'^2} = \sqrt{\xi^2 + \eta^2} = (\omega/C_p) \sqrt{\ell^2 + m^2}$$

$$r = in/\sqrt{\ell^2 + m^2} = \sqrt{1 - (\omega/kC_p)^2}$$

$$s = in'/\sqrt{\ell'^2 + m'^2} = \sqrt{1 - (\omega/kC_s)^2}$$

$$p = \ell/\sqrt{\ell^2 + m^2} = \ell'/\sqrt{\ell'^2 + m'^2} = \xi/k$$

$$q = m/\sqrt{\ell^2 + m^2} = m'/\sqrt{\ell'^2 + m'^2} = \eta/k$$

$$\alpha = C_s/C_p = \sqrt{(1 - 2\nu)/2(1 - \nu)}$$

A_p, A_{SH}, A_{SV} are then the amplitudes of waves travelling in the positive z direction; A_p', A_{SH}', A_{SV}' are the amplitude of waves travelling in the negative z direction.

The stresses $\tau_{xz}, \tau_{yz}, \sigma_z$ are given by

$$\tau_{xz} = G \gamma_{xz} = G (\partial u/\partial z + \partial w/\partial x)$$

$$\tau_{yz} = G \gamma_{yz} = G (\partial v/\partial z + \partial w/\partial y)$$

$$\sigma_z = \lambda e + 2G \epsilon_z = \lambda \partial u/\partial x + \lambda \partial v/\partial y + (\lambda + 2G) \partial w/\partial z$$

and can be expressed as

8

$$S = \begin{Bmatrix} \frac{\tau_{xz}}{2kG} \\ \frac{\tau_{yz}}{2kG} \\ \frac{i\sigma_z}{2kG} \end{Bmatrix} = \begin{bmatrix} -rp & sq/2 & -\frac{p(1+s^2)}{2} & rp & -sq/2 & -\frac{q(1+s^2)}{2} \\ -rq & -sp/2 & \frac{q(1+s^2)}{2} & rq & sp/2 & -\frac{q(1+s^2)}{2} \\ -(\frac{1+s^2}{2}) & 0 & -s & -\frac{(1+s^2)}{2} & 0 & s \end{bmatrix} E_z Af$$

Choosing a local system of coordinates for the layer with $z = 0$ at the top and $z = -h$ (layer thickness) at the bottom the displacements and tractions at the 2 layer interfaces can be written as

$$\begin{aligned} U_0 &= CAF \\ U_{-h} &= CE_{-h}AF \\ \begin{Bmatrix} U_0 \\ U_{-h} \end{Bmatrix} &= \begin{bmatrix} C \\ CE_{-h} \end{bmatrix} AF \\ T_0 &= S_0 = DAF \\ T_{-h} &= -S_{-h} = -DE_{-h}AF \\ \begin{Bmatrix} T_0 \\ T_{-h} \end{Bmatrix} &= \begin{bmatrix} D \\ -DE_{-h} \end{bmatrix} AF \end{aligned}$$

Leading to

$$AF = \begin{bmatrix} C \\ CE_{-h} \end{bmatrix}^{-1} \begin{Bmatrix} U_0 \\ U_{-h} \end{Bmatrix}$$

and

$$\begin{Bmatrix} T_0 \\ T_{-h} \end{Bmatrix} = \begin{bmatrix} D \\ -DE_{-h} \end{bmatrix} \begin{bmatrix} C \\ CE_{-h} \end{bmatrix}^{-1} \begin{Bmatrix} U_0 \\ U_{-h} \end{Bmatrix} = K \begin{Bmatrix} U_0 \\ U_{-h} \end{Bmatrix}$$

The matrix K is the stiffness matrix of the layer, function of the wave numbers ξ , η .

Assembling the stiffness matrices of the various layers the matrix of the complete soil profile can be obtained. When the bottom of the profile can be assumed to be rigid $U_h = 0$ for the last layer and only the top 3×3 submatrix of the stiffness K for the last layer is used. When the bottom is an elastic half-space if the excitation results from forces applied on the layers there are no incoming waves travelling in the positive z direction through the half-space. Making then A_p , A_{SH} and A_{SV} equal to 0 and keeping the last three columns of the matrices C , D

$$U_0 = C_2 AF$$

$$T_0 = D_2 AF$$

$$T_0 = D_2 C_2^{-1} U_0 = K U_0$$

K is the stiffness matrix for a half-space relating forces to displacements at the surface.

Once the total stiffness matrix has been assembled

$$KU = P$$

U are the displacements at the layers interfaces and P are forces applied at the same levels. If these forces are of the form $p(x,y)$ it is necessary to obtain first

$$P(\xi,\eta) = 1/4\pi^2 \int_{-\infty}^{\infty} \int_{-\infty}^{\infty} P(x,y) e^{i\xi x} e^{i\eta y} dx dy$$

The displacements in the wave number domain (in terms of ξ, η) are then

$$U(\xi,\eta) = K^{-1}P(\xi,\eta)$$

Finally the displacements as a function of x,y are

$$U(x,y) = \int_{-\infty}^{\infty} \int_{-\infty}^{\infty} U(\xi,\eta) e^{-i\xi x} e^{-i\eta y} d\xi d\eta$$

The determination of the steady state displacements due to a harmonic load applied at the surface (or any interface) of a horizontally layered soil deposit requires therefore the decomposition of the load into its ξ, η components (equivalent to a double Fourier series), the assembly of the stiffness matrix of the profile for each set of values ξ, η ; the solution of the system of equations $KU = P$ and the inverse transform from ξ, η (wave number domain) to x, y (space domain). The most delicate part of this process is the last one with the numerical evaluation of the double integral.

2.3 Plane Waves

When the directions of propagation of the waves are all in one plane it can be assumed without loss of generality that this is the $x-z$ plane. Making then $m = 0$ in the above expressions the in plane motions (u,w) and stresses (σ_z, τ_{xz}), caused by P and SV waves, can be uncoupled from the out of plane motion v and stresses τ_{yz} , caused by SH waves. Only one wave number k is then needed for the solution with

$$k = \omega l / C_p = \omega l' / C_s = \xi$$

$$p = 1, q = 0 = \eta$$

Explicit expressions for the stiffness matrices corresponding to in plane and out of plane motions have been presented by Kausel and Roesset (Ref 14).

2.4 Wave Equations in Cylindrical Coordinates

The radial, tangential and vertical displacements u , v , w in cylindrical coordinates can be expressed in the form

$$u = \sum_{m=0}^{\infty} (u_{ms} \cos m\theta + u_{ma} \sin m\theta)$$

$$v = \sum_{m=0}^{\infty} (-v_{ms} \sin m\theta + v_{ma} \cos m\theta)$$

$$w = \sum_{m=0}^{\infty} (w_{ms} \cos m\theta + w_{ma} \sin m\theta)$$

which represents an expansion in Fourier series in the circumferential direction. u_{ms} , v_{ms} , w_{ms} represent symmetric and u_{ma} , v_{ma} , w_{ma} antisymmetric components. An advantage of the expression is that for many practical problems only one term is needed. Thus for instance when dealing with a vertical load uniformly distributed over a circular area (the case of primary interest for the present work) only the symmetric term with $m = 0$ is needed and

$$u = u_0 \cos \theta$$

$$v = 0$$

$$w = w_0 \cos \theta$$

The wave equations in terms of the volumetric strain and the rotation vector are independent of the system of coordinates and apply equally to cylindrical coordinates. A general solution for the symmetric or antisymmetric components of the displacements for a given value of m is then given by

$$U_m = \begin{Bmatrix} u \\ v \\ w \end{Bmatrix} = \begin{Bmatrix} \frac{d}{dr} C_m & \frac{m}{r} C_m & 0 \\ \frac{m}{r} C_m & \frac{d}{dr} C_m & 0 \\ 0 & 0 & -kC_m \end{Bmatrix} C E_z A = F_m C E_z A = F_m \bar{U}_m$$

where C is the same matrix of cartesian coordinates for the plane wave case ($p = 1$, $m = m' = q = \eta = 0$, $k = \xi$).

$C_m = C_m(kr)$ are cylindrical functions of m th order and first, second or third kind (Bessel, Neumann or Hankel functions respectively). Hankel functions are often used because they behave asymptotically like complex exponentials.

First Hankel functions are used to model waves travelling from infinity towards the origin, and second Hankel functions for waves travelling from the center region towards the farfield. These functions show, however, a singularity for zero argument and cannot be used if the problem includes the origin.

The stresses $S_m = (\tau_{rz}, \tau_{r\theta}, \sigma_z)^T$ can be expressed in the form

$$S_m = 2kGF_m D E_z A = F_m \bar{S}_m$$

Where the F_m matrix is the same defined above for the displacements, with terms involving cylindrical functions of m th order and D is the same matrix defined for cartesian coordinates applied to the plane case ($q = 0, p = 1$).

One can again form a stiffness matrix for the layer relating tractions resulting from the stresses S at both interfaces and the displacements U . It must be noticed that these matrices are a function of the wave number k but they are independent of m and are therefore the same for all terms of the Fourier series expansion.

The problem of a load applied at the free surface or any interface can then be solved in cylindrical coordinates by obtaining

$$\bar{P}_m = a_m \int_0^\infty r F_m \int_0^{2\pi} T_m P(r, \theta) dr d\theta$$

with F_m as defined above and

$T_m = \text{diag}(\cos m\theta, -\sin m\theta, \cos m\theta)$ for symmetric loads with respect to the x axis.

$T_m = \text{diag}(\sin m\theta, \cos m\theta, \sin m\theta)$ for antisymmetric loads with respect to the x axis.

The displacements

$$\bar{U}_m = K^{-1} \bar{P}_m, U = \sum_{m=0}^{\infty} T_m \int_0^\infty k F_m \bar{U}_m dk$$

are obtained by assembling the stiffness matrix of the profile and solving the system of equations.

The most delicate part of this procedure is again the numerical evaluation of the integral from 0 to ∞ to convert the displacements from the wave number domain (function of k) to the space domain (function of r and θ).

2.5 Discrete Model

Assuming that the layers are relatively thin an approximate finite element type solution can be obtained assuming that the variation of the displacements with depth is given by

$$U = -(z/h) U_{\text{bot}} + (1 + z/h) U_{\text{top}}$$

One could, of course, use a quadratic variation or any other polynomial, but the linear variation implied by the above formula is used here.

It is then possible to obtain a stiffness matrix for the layer (plane wave or cylindrical coordinates) of the form

$$K = A k^2 + B k + C - \omega^2 M$$

as reported by Waas (1972), Kausel (1974), and Kausel and Roesset (1981). k is again the wave number.

The matrices A , B , C and M involve only the material properties of the layer. The main advantage is that this stiffness matrix does not involve transcendental functions of k . It is possible then to assemble the total stiffness matrix of the soil deposit and proceed with the solution as in the continuous formulation.

Considering instead the case where no loads are applied

$$(A k^2 + B k + C - \omega^2 M) X = 0$$

This system of equations represents a quadratic eigenvalue problem. The eigenvalues k and the eigenvectors X are the wave numbers and the mode shapes of the waves propagating in the soil at a frequency ω .

This problem yields $6N$ eigenvalues k_j and eigenvectors X_j if N is the total number of layers (assuming a rigid bottom). $3N$ of these correspond to eigenvalues k_j and shapes X_j , while the other half are eigenvalues $-k_j$ and shapes X'_j (X'_j is obtained from X_j by changing the sign of the vertical components). Following Waas one chooses the $3N$ modes that have eigenvalues k_j whose imaginary part is negative if k_j is complex, or whose real part is posi-

tive if k_j is real. These are the modes that decay with distance from the source. An efficient solution of the eigenvalue problem has been presented by Kausel (1981).

$2N$ of the modes have zero v displacements and correspond to generalized Rayleigh waves. The other N modes have zero u and w displacements and correspond to generalized Love waves.

Calling U_j the u components of X_j and W_j the w components and V_j the eigenvectors with only v components the flexibility matrix of the total soil deposit (Inv. K) can be expressed directly in terms of the eigenvectors and eigenvalues as

$$K^{-1} = \begin{Bmatrix} f_{uu} & 0 & f_{uw} \\ 0 & f_{vv} & 0 \\ f_{wu} & 0 & f_{ww} \end{Bmatrix}$$

The submatrices f_{uu} , f_{uw} etc. are of order $N \times N$. Their general terms $f_{uu}(m,n)$ (m th row, n th column) are given according to Kausel (1981) by

$$f_{uu}(m,n) = \sum_{j=1}^{2N} U_{jm} U_{jn} a_j$$

$$f_{uw}(m,n) = \sum_{j=1}^{2N} U_{jm} W_{jn} b_j$$

$$f_{wu}(m,n) = \sum_{j=1}^{2N} W_{jm} U_{jn} b_j$$

$$f_{ww}(m,n) = \sum_{j=1}^{2N} W_{jm} W_{jn} a_j$$

$$f_{vv}(m,n) = \sum_{j=1}^{2N} V_{jm} V_{jn} a_j$$

where U_{jm} represents the m th component of U_j etc.

$$a_j = 1/(k^2 - k_j^2)$$

$$b_j = k/[k_j(k^2 - k_j^2)]$$

The displacements U can then be obtained from the forces P multiplying them by the flexibility matrix Inv. K . The main advantage of this formulation is that the integrals involved in the transformation from the space to the wave number domain and vice versa can be evaluated explicitly.

For the case of a uniform vertical disk load q applied over a disk of radius R , of particular interest for this study

$$\begin{aligned}\bar{p} &= 1/2\pi \int_0^R \int_0^{2\pi} r F_o T_o P d\theta dr \\ &= 1/2\pi q \int_0^R r F_o \int_0^{2\pi} \begin{Bmatrix} 0 \\ 0 \\ 1 \end{Bmatrix} d\theta dr \\ &= qR/k J(kR) \begin{Bmatrix} 0 \\ 0 \\ -1 \end{Bmatrix}\end{aligned}$$

(only the $m = 0$ term is involved).

The displacements at the i th interface due to a vertical disk load at the j th interface are then

$$\bar{U} = F\bar{P}$$

and

$$U = T_o \int_0^\infty k F_o U dk$$

leading to

$$u = qR \sum_{\ell=1}^{2N} U_{\ell i} W_{\ell j} I_{2\ell} / k_\ell$$

$$v = 0$$

$$w = qR \sum_{\ell=1}^{2N} W_{\ell i} W_{\ell j} I_{1\ell}$$

with

$$I_{1\ell} = \pi/2 i k_\ell J_0(k_\ell r) H_1^{(2)}(k_\ell R) - 1/R k_\ell^2 \quad 0 \leq r \leq R$$

$$= \pi/2 i k_{lit} J_1(k_\ell R) H_0^{(2)}(k_\ell r) \quad r \geq R$$

and

$$\begin{aligned}
 I_{2\ell} &= \pi/2i J_1(k_\ell r) H_1^{(2)}(k_\ell R) \quad 0 \leq r \leq R \\
 &= \pi/2i J_1(k_\ell R) H_1^{(2)}(k_\ell r) \quad r \geq R
 \end{aligned}$$

The more detailed derivation and a complete set of expressions for other loads can be found in Kausel's work (Ref 13).

The main advantage of Kausel's formulations is that the numerical integrations are avoided since the results are expressed explicitly in terms of Bessel and Hankel functions and the modal shapes of the waves in the soil deposit. The drawback is that the soil profile must be divided into very thin layers (due to the linear approximation to the variation of displacements with depth) in order to get accurate results. This is not a serious limitation when the soil properties vary with depth and many layers are needed in any case to reproduce properly the variation of the elastic moduli. It makes the method less attractive when dealing with a homogeneous half-space or a very deep homogeneous soil stratum. The thickness of the layers needed to get good results was explored in this work through a series of parametric studies and rules to generate automatically an appropriate mesh were derived.

Another limitation of this approach is the assumption of a rigid bottom at a finite depth, implied in the solution of the eigenvalue problem. In the continuous formulation an underlying homogeneous half-space is accounted for using a stiffness matrix that relates forces and displacements at the top under the assumption that there are no waves propagating through the half-space in the positive z direction. Kausel (1981) has suggested an approximation to simulate the half-space expanding the continuum stiffness matrix.

$$K = 2kG \left\{ \frac{1-s^2}{2(1-rs)} \begin{Bmatrix} r & 1 \\ 1 & s \end{Bmatrix} - \begin{Bmatrix} 0 & 1 \\ 1 & 0 \end{Bmatrix} \right\} \quad \text{for in-plane motions}$$

$$K = kSG \quad \text{for out-of-plane motions}$$

leading to matrices A, B, C for the half-space of the form

$$A = \frac{1}{2} iG \frac{C_s}{w} \begin{bmatrix} 1 - 2\frac{C_p}{C_s} & 0 & 0 \\ 0 & -1 & 0 \\ 0 & 0 & (\frac{C_p}{C_s})^3 - 2(\frac{C_p}{C_s})^2 \end{bmatrix}$$

$$B = G \begin{bmatrix} 0 & 0 & \frac{C_p}{C_s} - 2 \\ 0 & 0 & 0 \\ \frac{C_p}{C_s} - 2 & 0 & 0 \end{bmatrix}$$

$$C = \frac{iw}{C_s} G \begin{bmatrix} 1 & 0 & 0 \\ 0 & 1 & 0 \\ 0 & 0 & \frac{C_p}{C_s} \end{bmatrix}$$

In this work both solutions, assuming a rigid base at some depth, and simulating a half-space through the approximate formulation, were implemented in a computer program and used for the studies described in the following chapters.

CHAPTER 3. SIMULATION OF DYNAFLECT TESTS

3.1 Introduction

The Dynaflect consists of a force generator and five geophones housed in a small trailer, which is towed by a light vehicle. The loading system consists of two counter-rotating eccentric masses. The resulting vertical force varies harmonically with time. At a frequency of 8 Hz a force of 1000 lbs is transmitted to the pavement through the loading wheels. The resulting deflection basin is measured by five geophones mounted on the trailer draw bar at 12-inch intervals. The position of the geophones (stations) with respect to the wheels is shown schematically in Figure 3.1. The deflections measured represent the amplitudes of the steady state displacements at a given frequency (8 Hz). They are interpreted, however, as static displacements, assuming that the subgrade is homogeneous and extends to infinity.

3.2 Application to a Pavement System

A pavement system was selected to evaluate the importance of dynamic effects on the results of the Dynaflect tests. The pavement has a thickness of 2.5 inches and a Young's modulus of 200 ksi. The soil of the subgrade was considered both homogeneous with a Young's modulus of 29 ksi, and with a modulus starting with this value at the top and increasing with depth. Different depths to bedrock were used in the range from 10 to 110 feet. Displacements were computed at the points corresponding to the stations of the Dynaflect for a static load and for a frequency of 8 Hz. Figure 3.2 shows the profile and the meshes used for the study.

Figure 3.3 shows the variation of the static displacements with depth to bedrock at the five stations for the uniform subgrade. Notice that at station 1 (between the two wheels) the amplitude of the displacement varies from approximately 0.047 to 0.055 as the depth to bedrock increases from 10 to 110 ft, while at station 5 it changes from 0.007 to 0.014, illustrating the larger effect of the bottom soil layer on the response as the distance to the loaded area increases (all displacements must be multiplied by 10^{-6}). Figure 3.4 shows the corresponding results for a frequency of 8 Hz. It can be seen that two peaks appear at depths of approximately 35 and 42 ft, followed by a sharp valley.

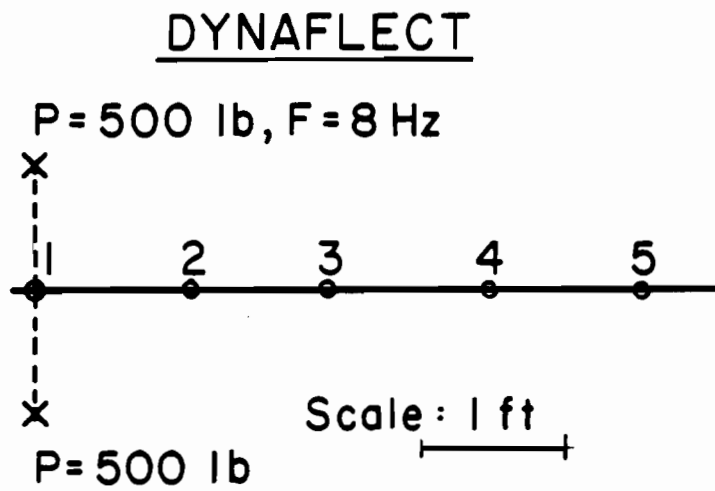


Fig. 3.1. Geometric Configuration of Loads and Stations for Dynaflect.

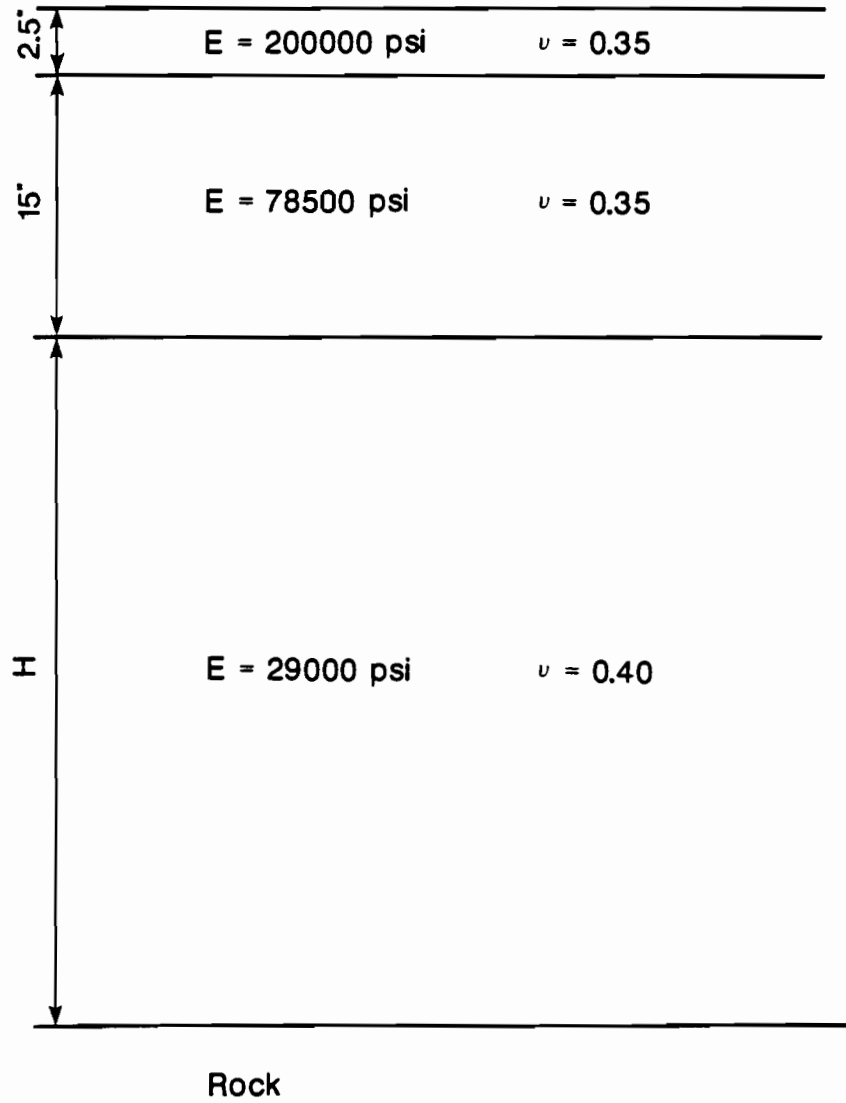


Fig. 3.2. Profile of Pavement Used for Studies.

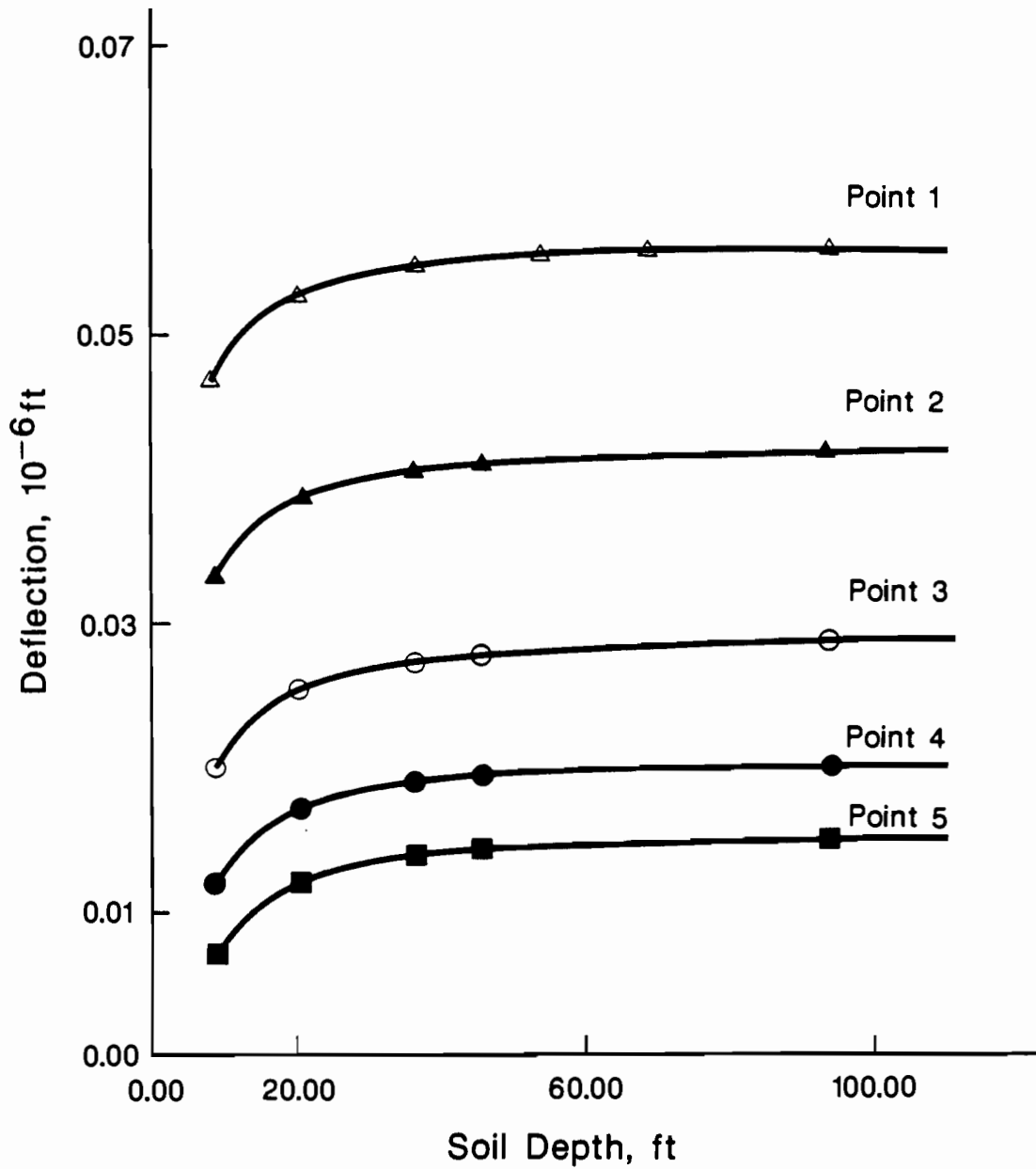


Fig. 3.3. Variation of Static Displacements with Depth to Bedrock - Dynaflect.

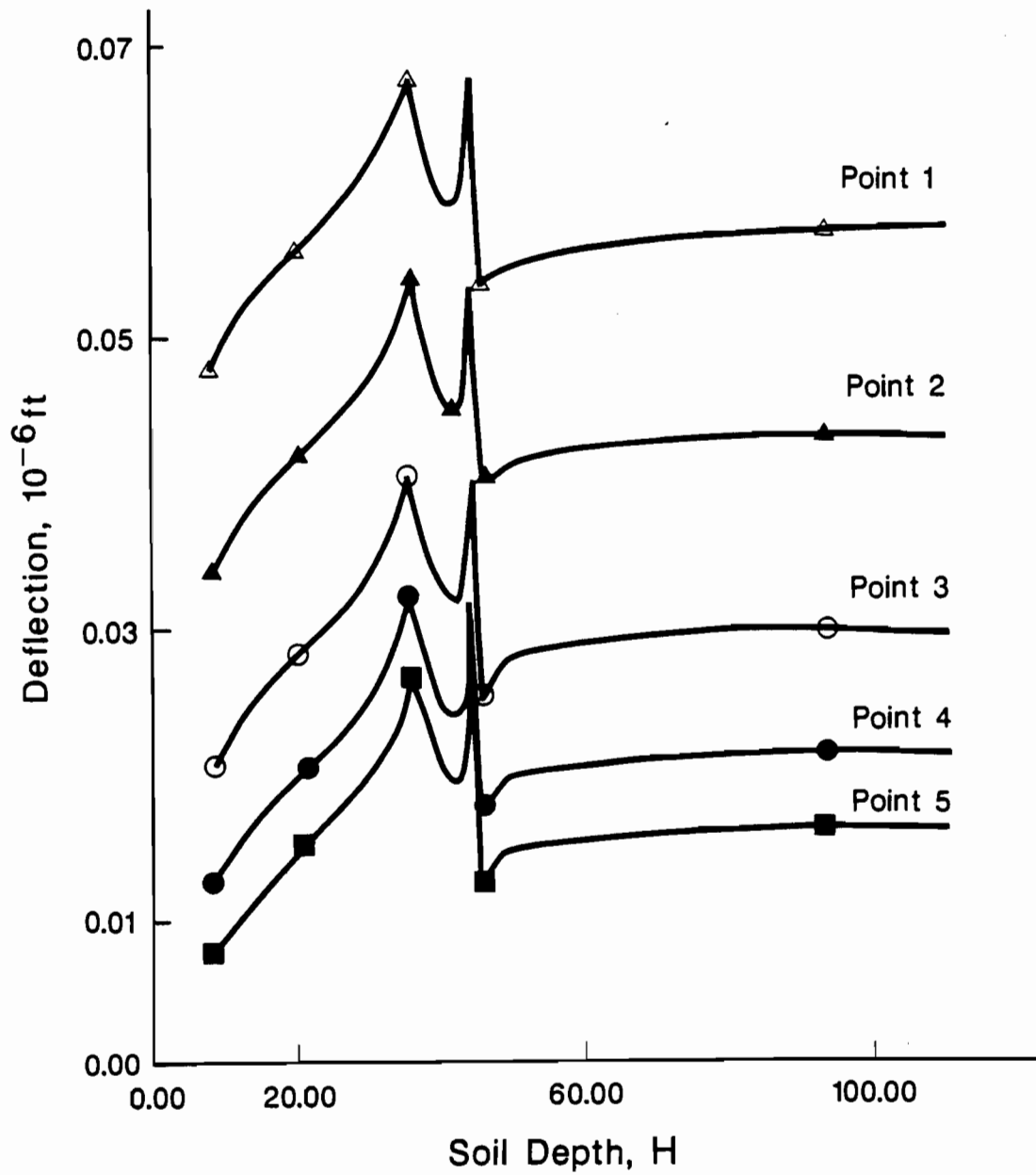


Fig. 3.4. Variation of Dynamic Displacements with Depth to Bedrock-Dynalect.

The ratio of the dynamic to the static displacements at points 1 and 5 is shown in Figure 3.5. The dynamic displacements are larger than the static ones in most cases, the only exception being the small range of depths to bedrock where a valley occurs. The maximum dynamic amplification occurs for a depth of the subgrade of about 35 feet. It is of the order of 1.25 at point 1 but increases with increasing distance reaching a value of nearly 2 at point 5. The range of depths over which there is a substantial dynamic amplification of the deflections is closely associated with the depths for which a frequency of 8 Hz represents the natural frequencies of the soil deposit in shear and dilatation.

Since the elastic properties of the pavement, base and subgrade are normally determined by comparing the measured deflections to those resulting from static analyses assuming that the sub-base is an elastic half-space it is more interesting to compare the dynamic results to the static deflections for an infinite depth to bedrock. The ratio of these deflections for points 1 and 5 is shown in Figure 3.6. These results indicate that for shallow depths to bedrock (less than 20 ft) the dynamic deflections are smaller than the static deflections for a half-space, although they are larger than the static deflections for the same soil profile with a finite depth. For a range of depths of 20 to 40 ft the dynamic results are larger than the static ones, the dynamic amplification being more pronounced as the distance to the load increases. The maximum amplification is now about 1.20 at point 1 and 1.75 at point 5. For depths larger than 50 or 60 ft the ratio of dynamic to static displacements is close to 1. It is thus for depths to bedrock less than 40 ft where the errors committed by the present interpretation procedures can be more serious for this particular profile. Larger depths would be significant if the soil of the subgrade were stiffer than the one selected.

Figures 3.7, 3.8 and 3.9 show the dynamic displacements and the ratios of dynamic to static displacements assuming 2 percent internal damping in the soil. It can be seen that introducing a small amount of material damping provides smoother curves, decreasing the amplitude of the peaks and eliminating almost completely the sharp valley at a depth of about 45 feet. The general conclusions remain, however, unchanged.

Figures 3.10 to 3.13 show the corresponding results when the modulus of the soil in the subgrade increases with depth, as is often the case in practice. The dynamic amplifications are somewhat smaller than those reported for the uniform subgrade but the range of depths over which dynamic effects are important is enlarged. Dynamic effects are significant in this case up to a depth

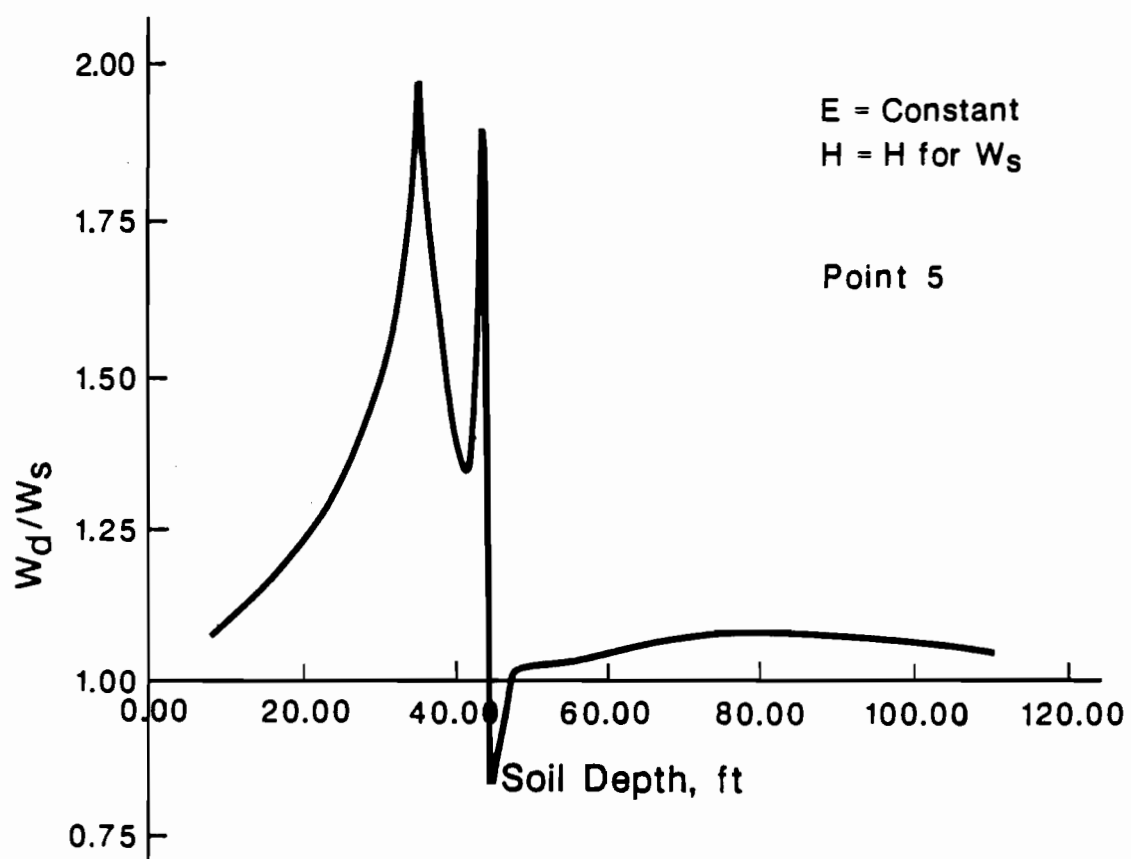
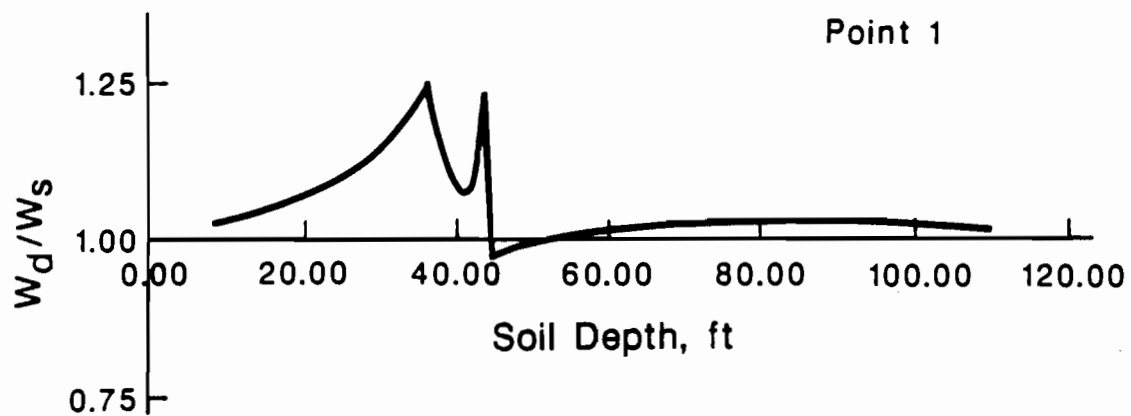


Fig. 3.5. Ratio of Dynamic to Static Displacements, Points 1 and 5 - Dynaflect.

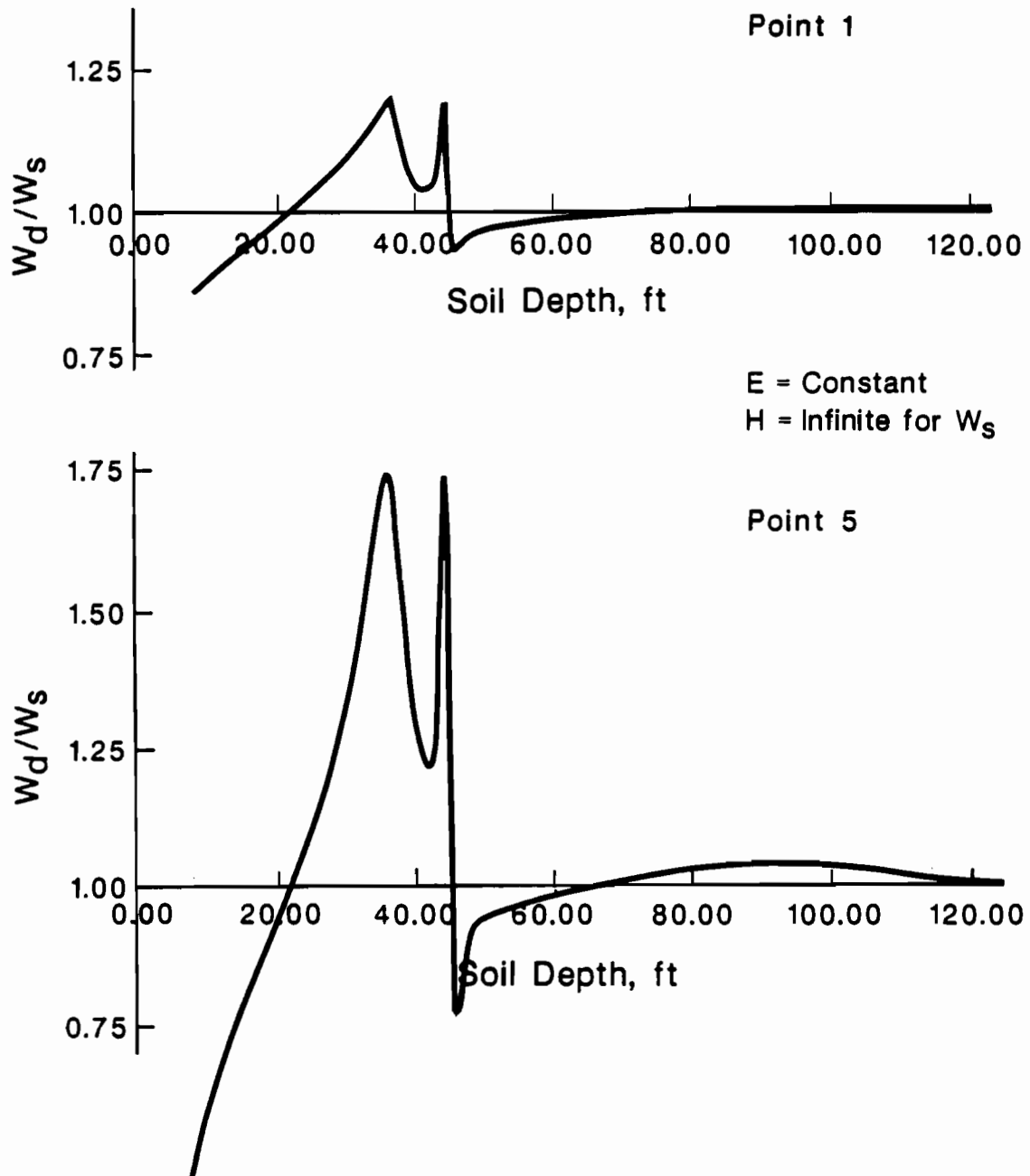


Fig. 3.6. Ratio of Dynamic to Static ($H = \infty$) Displacements, Points 1 and 5 - Dynaflect.

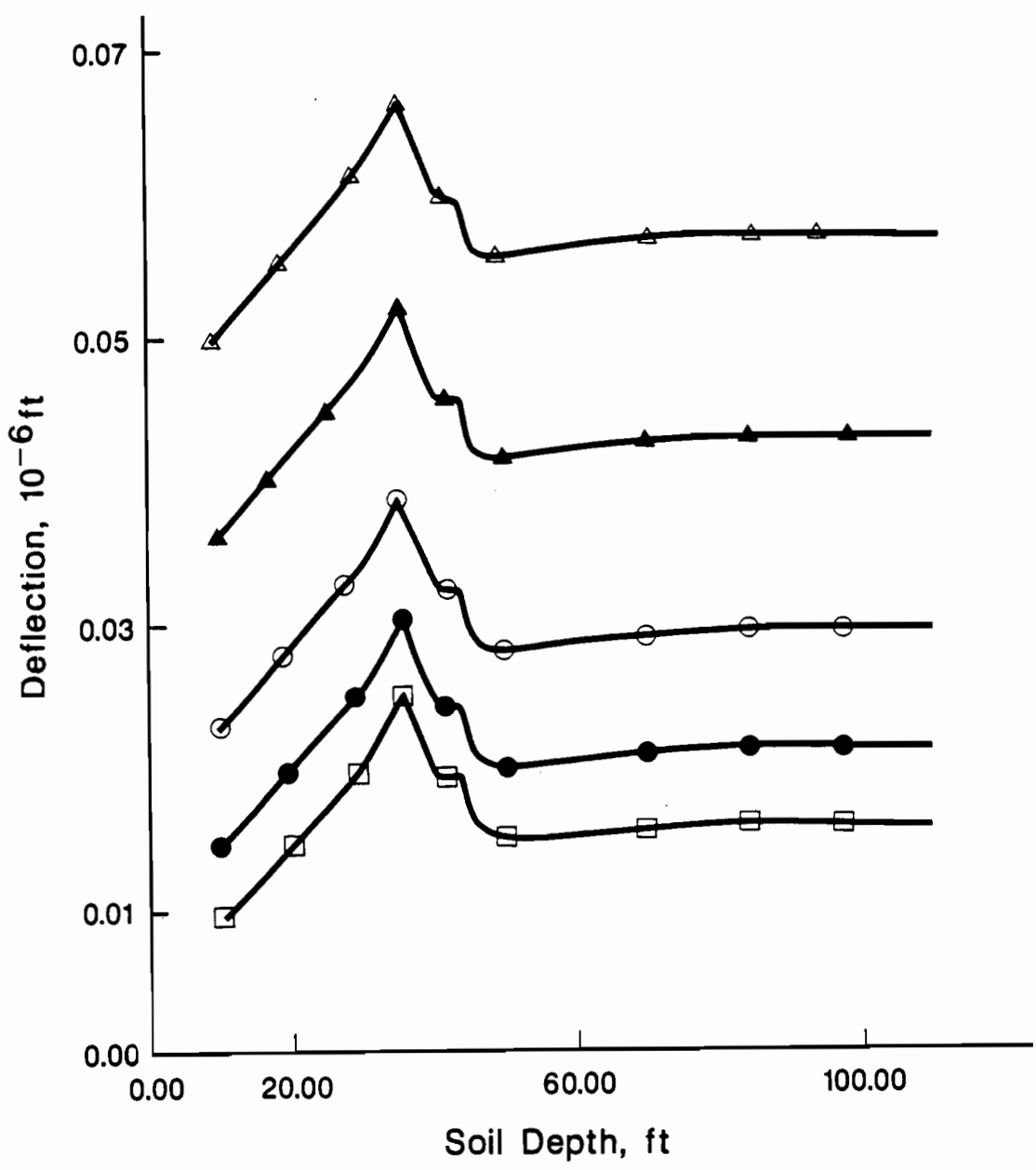


Fig. 3.7. Variation of Dynamic Displacements with Depth to Bedrock - Dynaflect, D = 0.02.

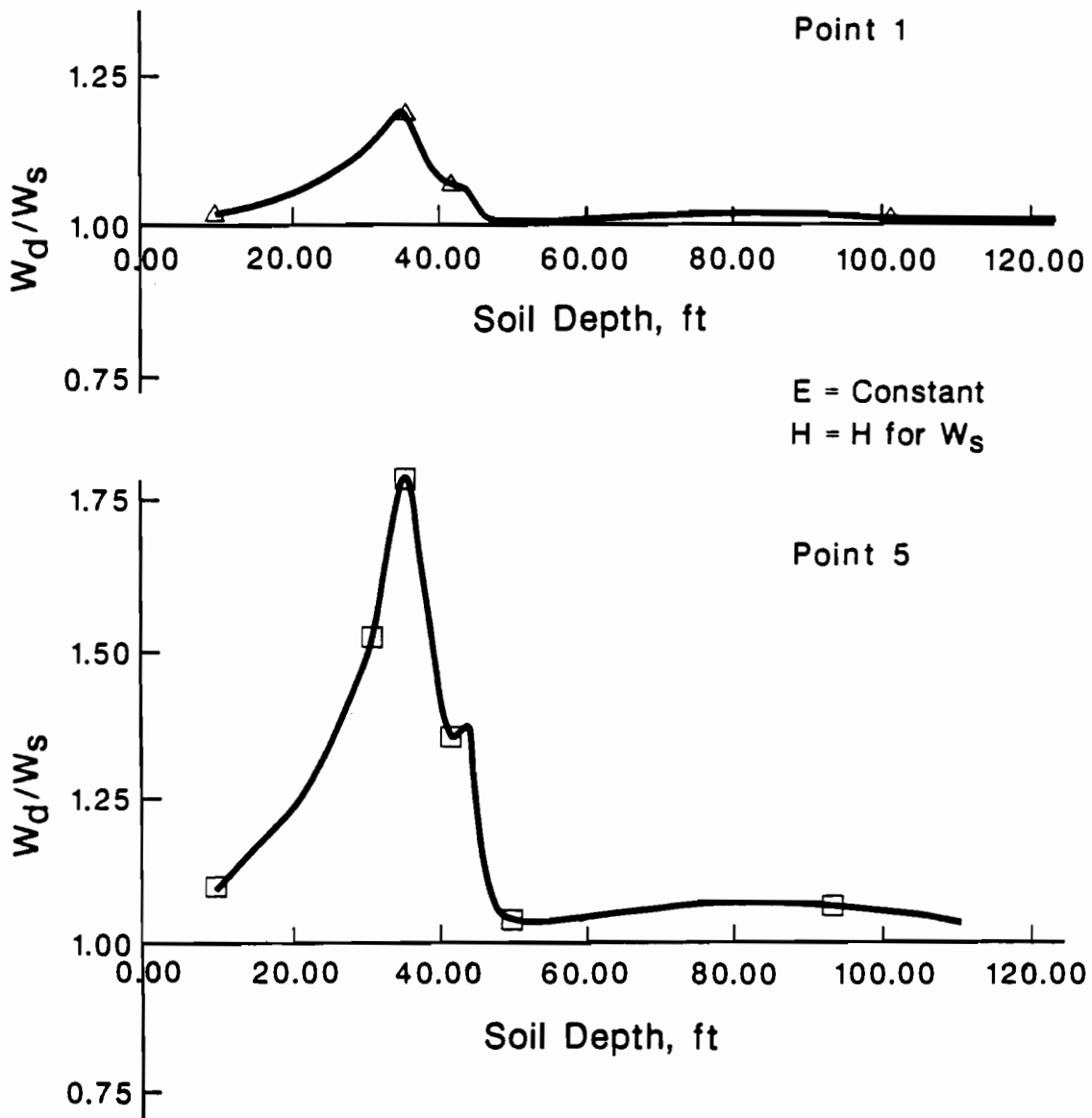


Fig. 3.8. Ratio of Dynamic to Static Displacements, Points 1 and 5, $D = 0.02$.

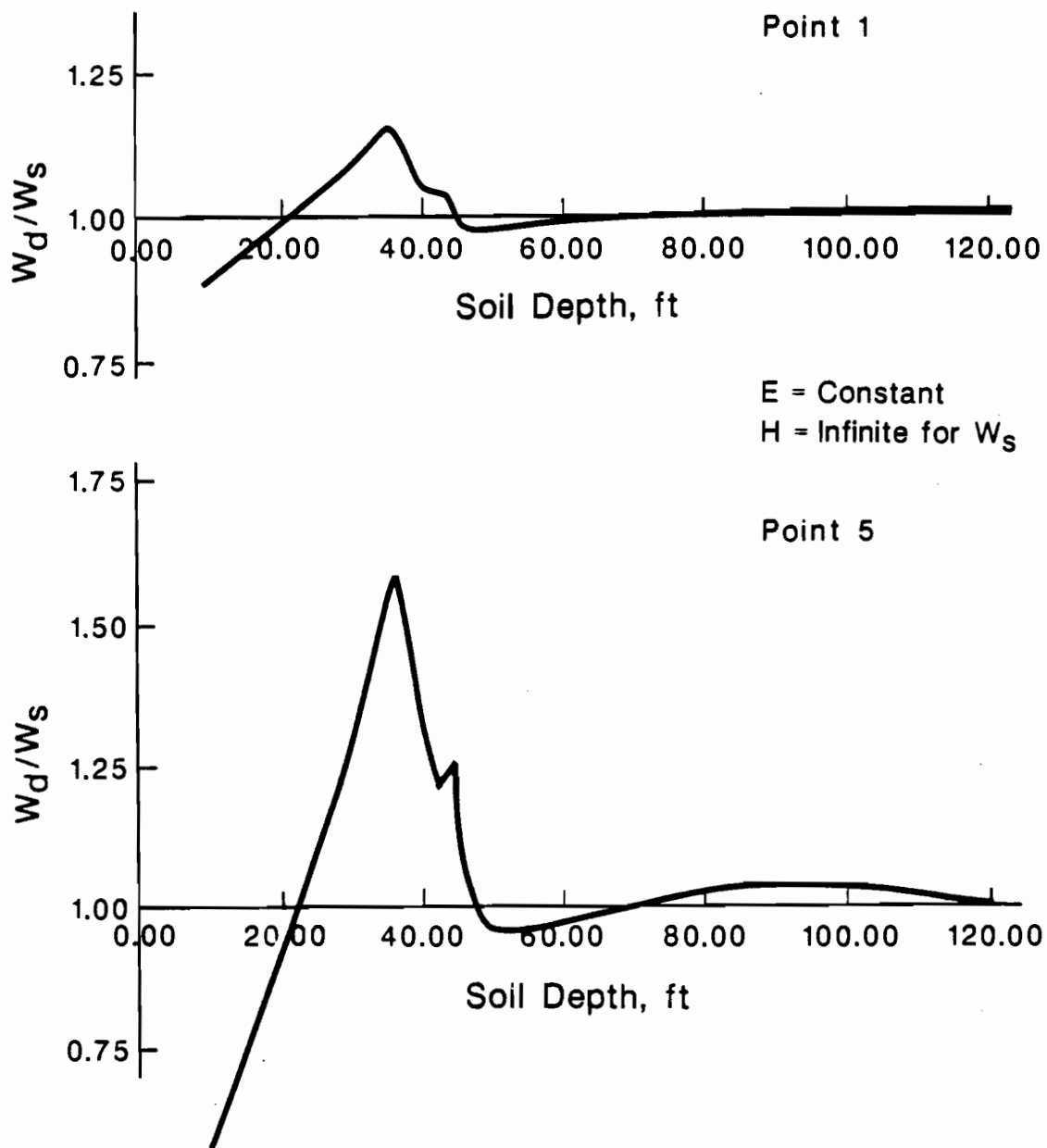


Fig. 3.9. Ratio of Dynamic to Static ($H = \infty$) Displacements, Points 1 and 5 - Dynaflect, $D = 0.02$.

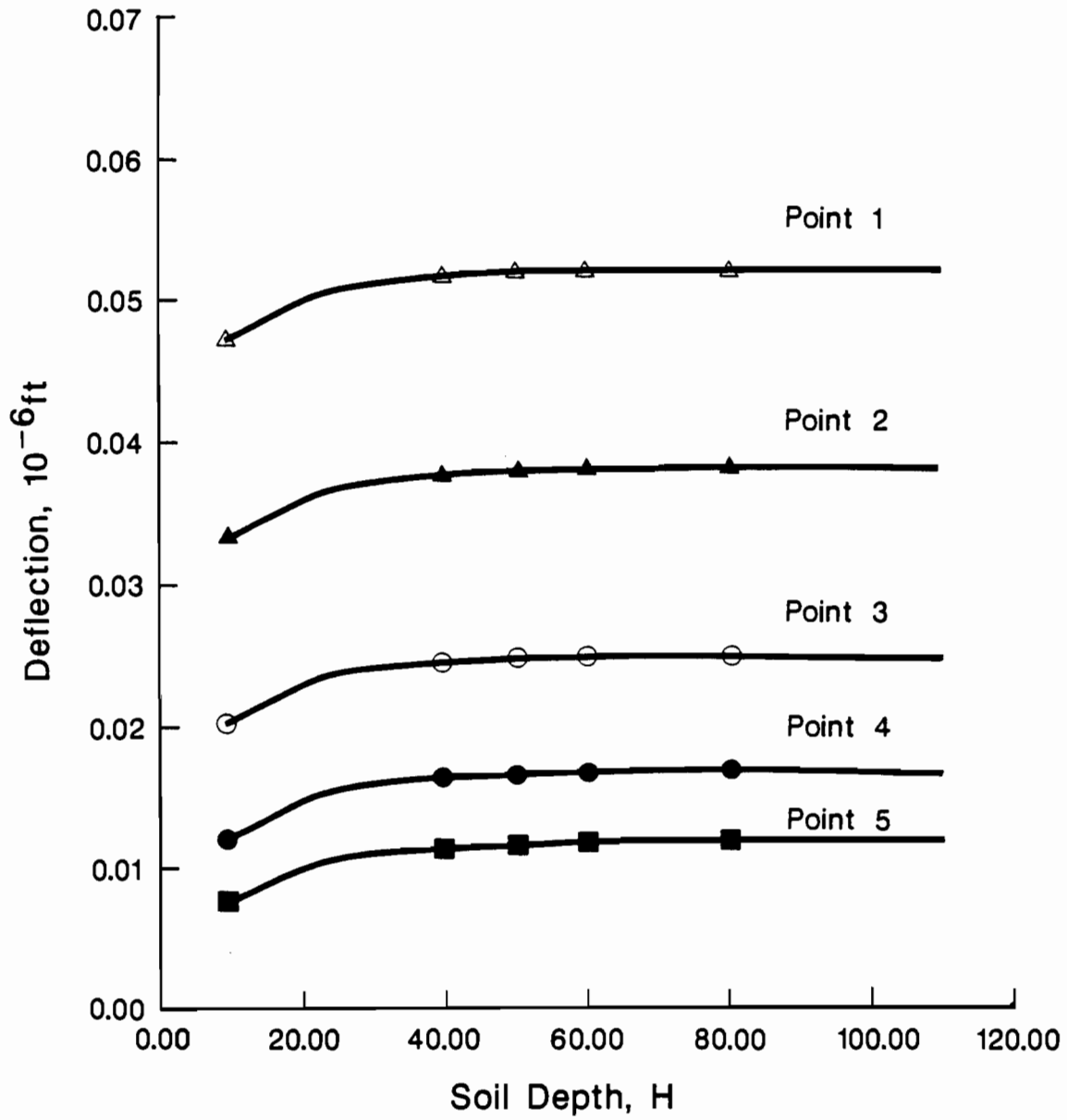


Fig. 3.10. Variation of Static Displacements with Depth to Bedrock - Dynaflect, G Inc.

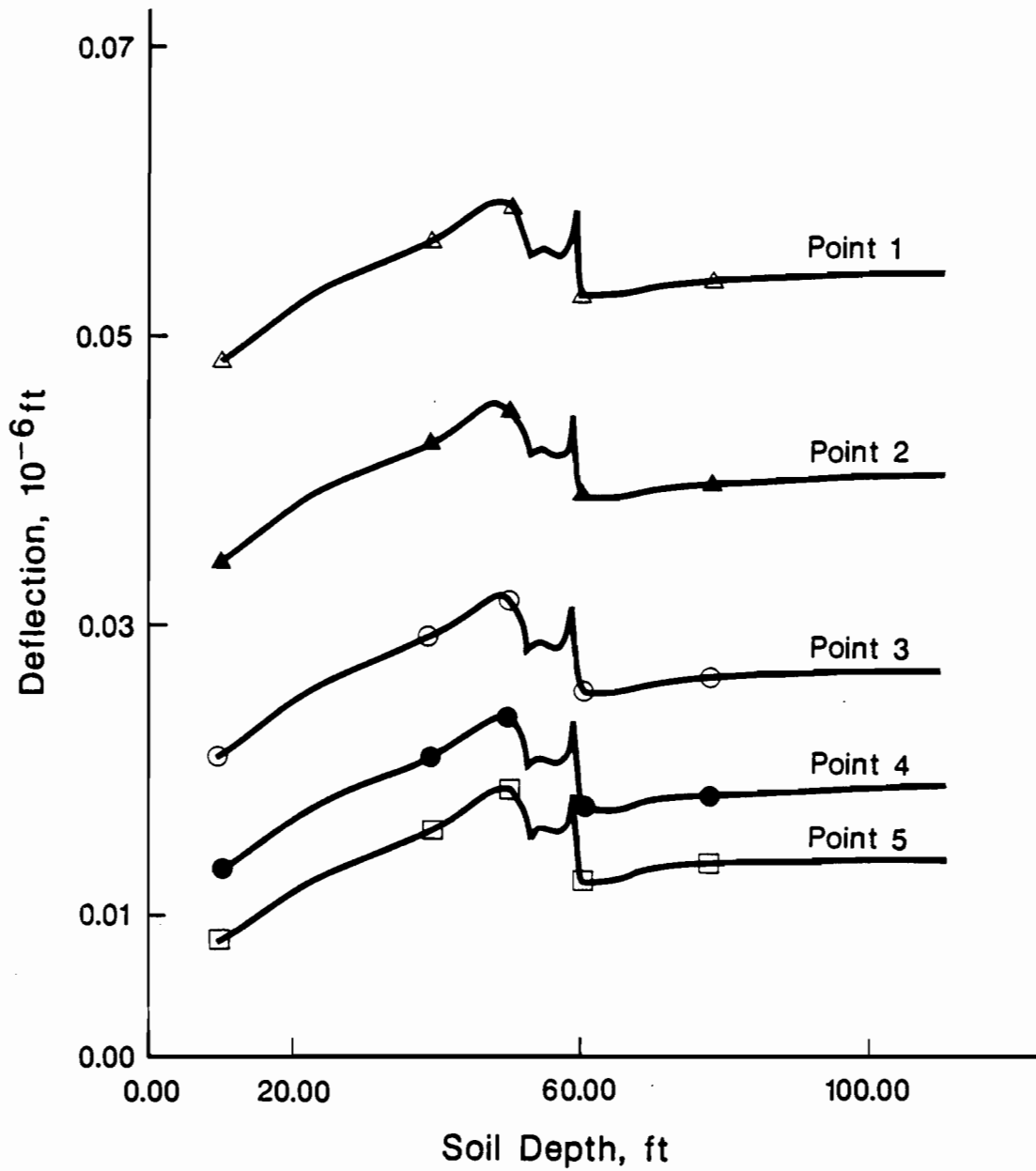


Fig. 3.11. Variation of Dynamic Displacements with Depth to Bedrock - Dynaflect, G Inc.

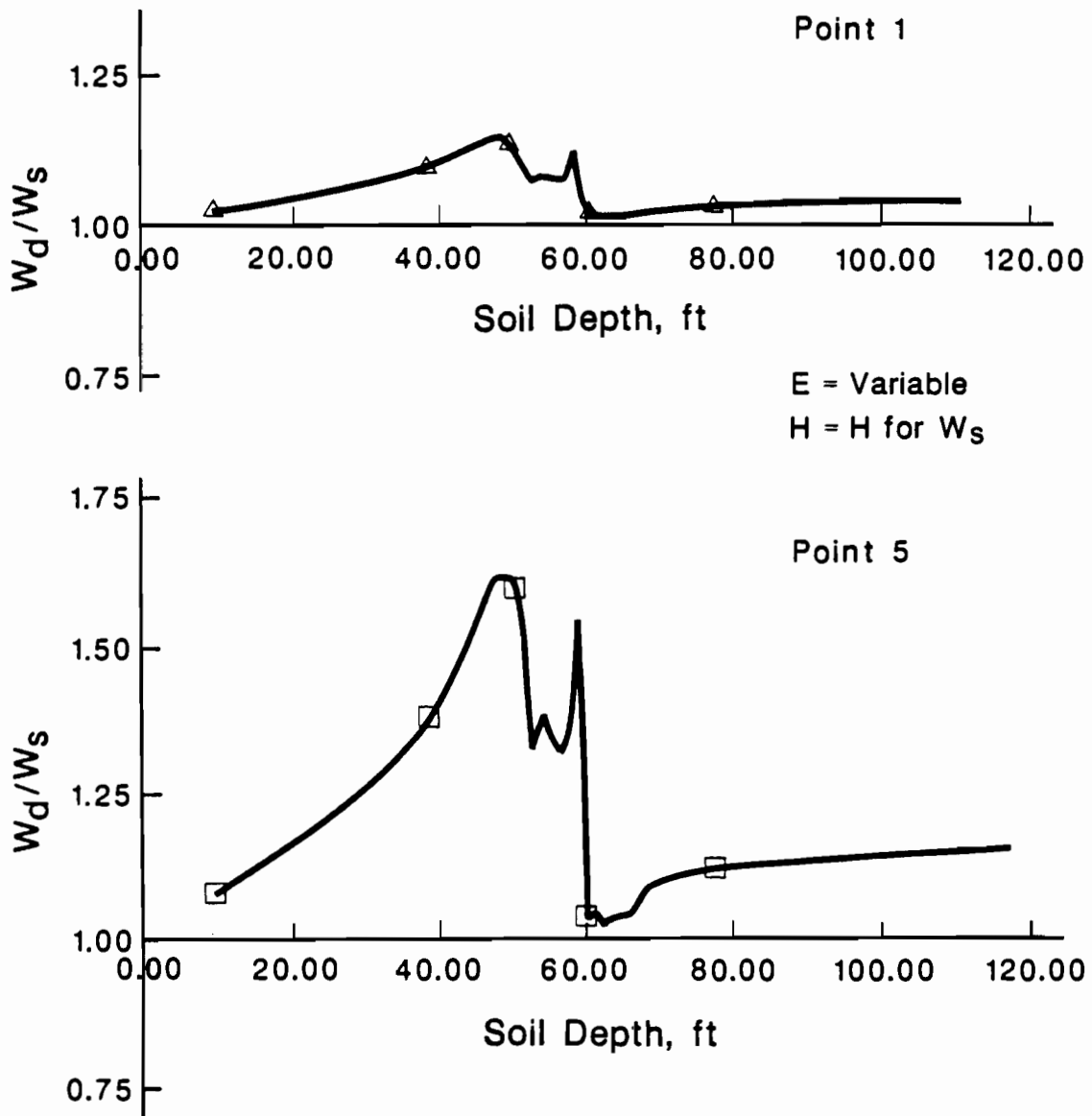


Fig. 3.12. Ratio of Dynamic to Static Displacements, Points 1 and 5, G Inc.

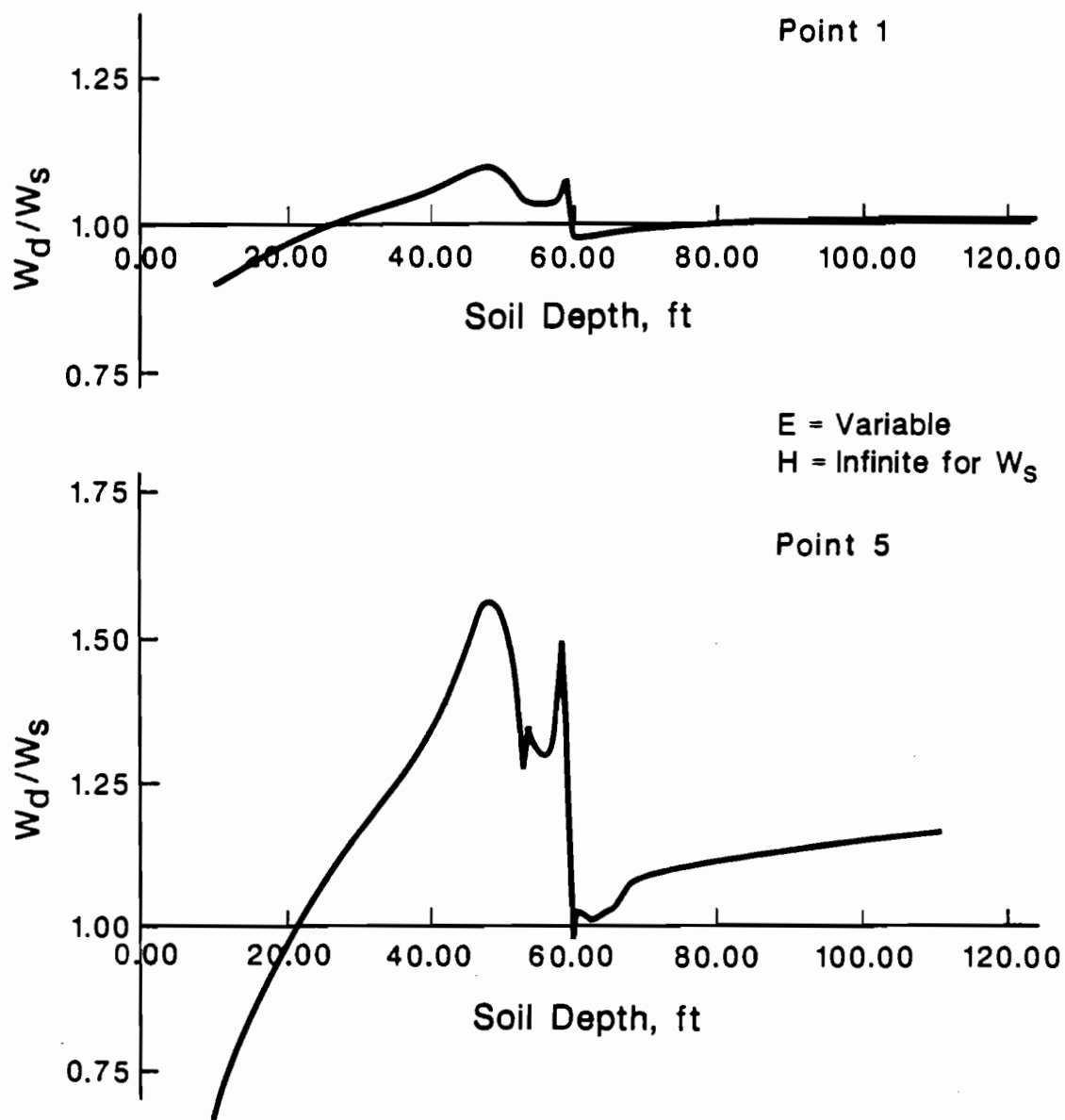


Fig. 3.13. Ratio of Dynamic to Static ($H = \infty$) Displacements for Variable Soil Profile - Dynaflect.

to bedrock of 60 feet. Moreover as the depth increases the ratio of the dynamic displacements to the static deflections assuming a uniform half-space does not tend to 1 as in the previous case. The values of this ratio at larger depths are affected by the distance of the station to the loaded area making the static interpretation of the results more difficult.

3.3 Estimation of Material Properties

Determination of the characteristics of the profile (elastic moduli of the pavement, base and subgrade) from the measured deflections falls into the general category of system identification problems (also referred to sometimes as the inverse problem). Because only five deflections are available, it is often assumed that the thickness of the pavement and the base are known, and that the only unknowns are the moduli of elasticity. These moduli are normally estimated by a trial and error procedure, assuming a set of values, computing the corresponding static deflections, comparing them to the measured values, and iterating until the differences are smaller than an acceptable tolerance. Unfortunately uniqueness of the solution cannot be guaranteed and different sets of elastic moduli can produce results which are within the specified tolerance.

To get a better feeling for the magnitude of the errors that can be committed when the moduli are computed using a static analysis the same hypothetical profile (Fig. 3.2) used for the previous studies was considered. Depths to bedrock of 10, 20, 35 and 110 ft were used as input. The amplitudes of the dynamic displacements at the five observation points corresponding to a harmonic force at a frequency of 8 Hz were then computed. These values are shown in Table 3.1 together with the static displacements for a subgrade which is an elastic half-space (depth to bedrock equal to infinity),

The computed dynamic displacements were then used as input to determine elastic moduli of the pavement, base and subgrade following a procedure similar to that used in practice today, starting with an assumed set of moduli (the actual values used for the dynamic analyses) and performing iterative linear analyses, adjusting the properties in each cycle, until the differences between the computed static deflections and the input values differed by less than a specified tolerance. The resulting predicted moduli are also shown in Table 3.1. If the displacements computed with the dynamic analyses for an assumed set of elastic moduli are assumed to simulate actual measurements the

TABLE 3.1. DEFLECTION BULBS AND PREDICTED ELASTIC MODULI FOR HOMOGENEOUS SUB-BASE AND DIFFERENT DEPTHS TO BEDROCK.

Displ. in (MILS)		Point 1	Point 2	Point 3	Point 4	Point 5	Young's Modulus (lb/in ²)	Errors (%)
Static	H=∞	0.70	0.52	0.36	0.26	0.20	200,000	
							78,500	
							29,000	
Dyn.	H=10ft	0.61	0.44	0.28	0.17	0.11	150,000	25.0
							30,000	61.8
							45,000	55.2
Dyn.	H=20ft	0.68	0.51	0.35	0.24	0.18	340,500	70.3
							78,000	0.6
							29,837	2.8
Dyn.	H=35ft	0.82	0.65	0.48	0.38	0.31	350,000	75.0
							98,500	25.5
							20,000	31.0
Dyn.	H=110ft	0.69	0.52	0.35	0.25	0.18	248,370	24.0
							78,500	0.0
							29,833	2.9

differences between the predicted values and those used for the dynamic computations can be interpreted as the errors that would be committed by ignoring dynamic effects. These differences, in percentage, are shown in Table 3.1 under the heading Errors. It can be seen that for a depth to bedrock of only 10 ft the stiffness of the sub-base is badly overestimated, while the modulus of elasticity of the base is underestimated as well as the modulus of the pavement. This results from the fact that the dynamic and finite layer effects are more pronounced for the farthest stations, whose deflections are heavily influenced by the soil properties at larger depths. For a depth to bedrock of 10 ft the properties of the base and the soil are accurately determined, but the modulus of the pavement is badly overestimated. For a depth of 35 ft the moduli of the pavement and the base are both overestimated while the stiffness of the sub-base is underestimated. This situation is the reverse of that encountered for a depth of 10 feet. When the depth of bedrock is 110 ft the results are more reasonable although the estimated modulus of the pavement is still 24 percent too high. It should be pointed out, again, that the solution is not unique and a different person might have computed different profiles.

CHAPTER 4. SIMULATION OF FALLING WEIGHT DEFLECTOMETER TESTS

4.1 Introduction

The Falling Weight Deflectometer has a 330.7 lb (150 kg) weight, mounted on a vertical shaft, housed in a compact trailer which can be easily towed by most conventional passenger cars. The weight is hydraulically lifted to a predetermined height (ranging from 0 to 15.7 inches or 0 to 400 mm). It is then dropped onto an 11.8-inch (300-mm)-diameter loading plate resting on a 0.22-inch (5.5-mm)-thick rubber pad which helps to distribute the load uniformly over the loading area. The resulting load is a force impulse with a duration of approximately 30 msec and a peak magnitude ranging from 0 to 14,000 lbs (0 to 60,000 Newtons), depending on the drop height. The displacements of various stations along the surface of the pavement (from the center of the loaded area to a point at a distance of 5 ft) are measured by velocity transducers. Figure 4.1 shows schematically the position of the load and the stations. The deflections measured are the peak displacements under a transient type dynamic excitation. The interpretation of the results to backfigure the elastic moduli is based again on static analyses assuming that the subgrade extends to infinity with uniform properties.

4.2 Determination of Transient Response

Since the loads applied by the Falling Weight Deflectometer are transient in nature, it is necessary, to simulate the results of this test, to decompose the time history of the force into frequency components using the Fourier transform. Figure 4.2 shows the time history of the applied load used for the present analyses (a triangular pulse with a duration of 33 milliseconds) and Figure 4.3 shows the amplitude of its Fourier transform. Analyses must then be conducted for a large number of different frequencies obtaining at each point (station) the transfer functions of the deflections. Figure 4.4 shows for example the transfer function at point 1 (center of the loaded area) for the pavement system of Figure 4.5 (same profile used for the Dynaflect studies) and a depth to bedrock of 20 feet. These transfer functions are then multiplied by the Fourier transform of the input and the resulting functions are converted back to time using the Inverse Fourier Transform. The final results are the

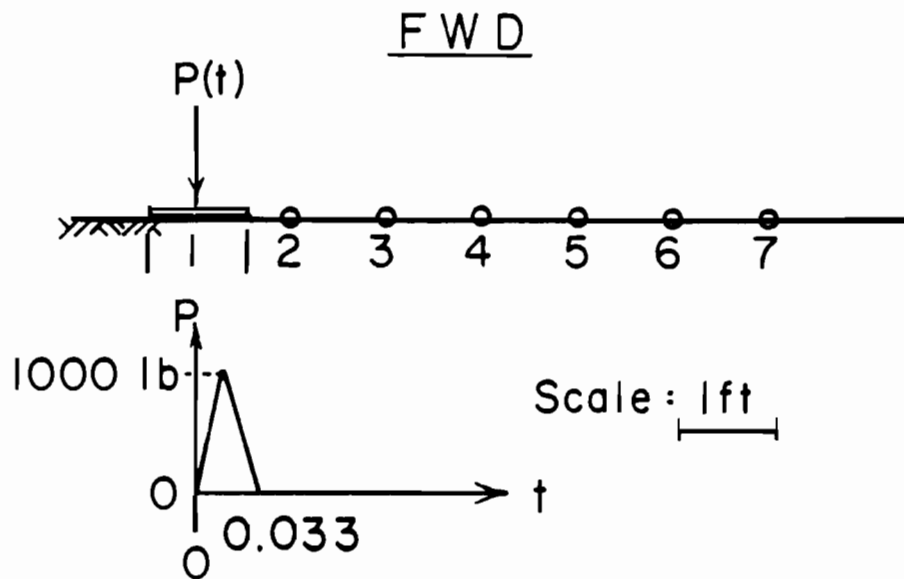


Fig. 4.1. Geometric Configuration of Loads and Stations for Dynaflect and Falling Weight Deflectometer.

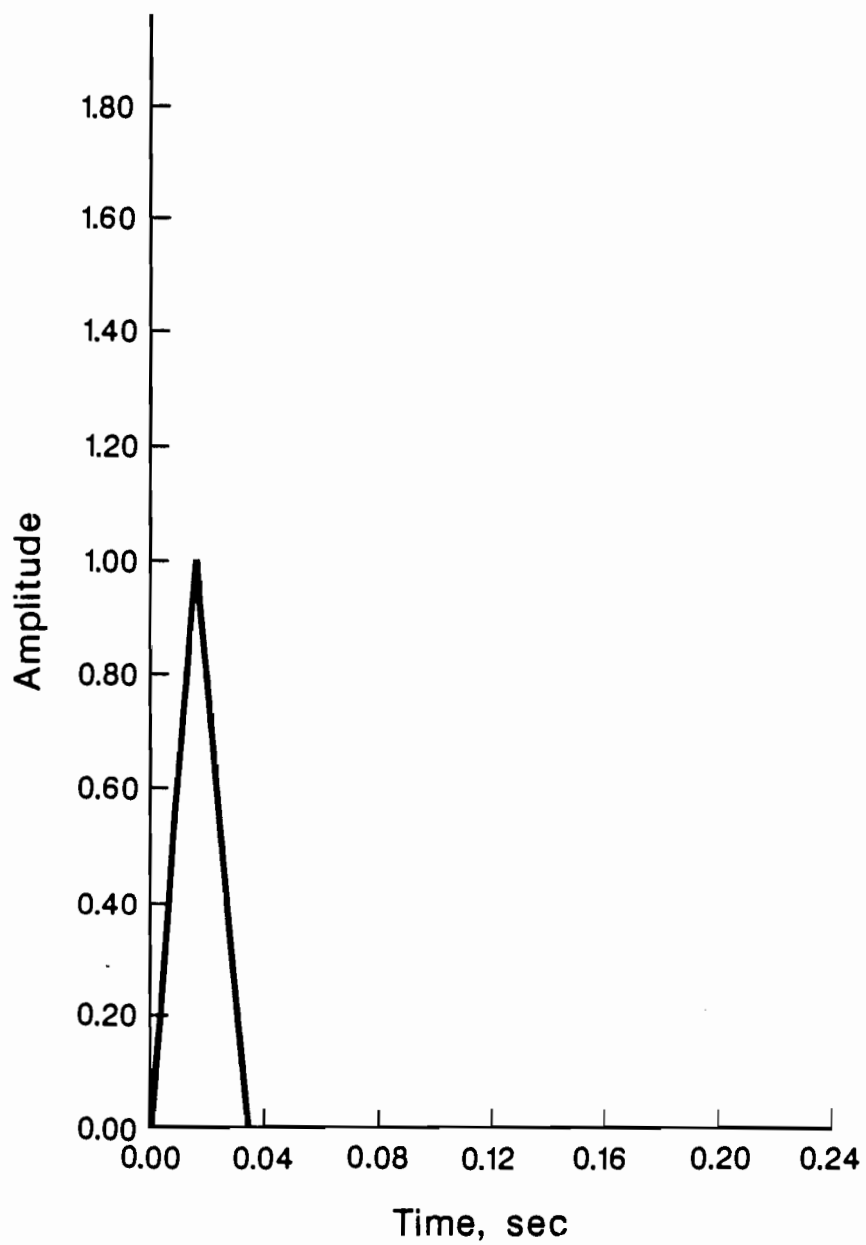


Fig. 4.2. Time History of Imuplse Load.

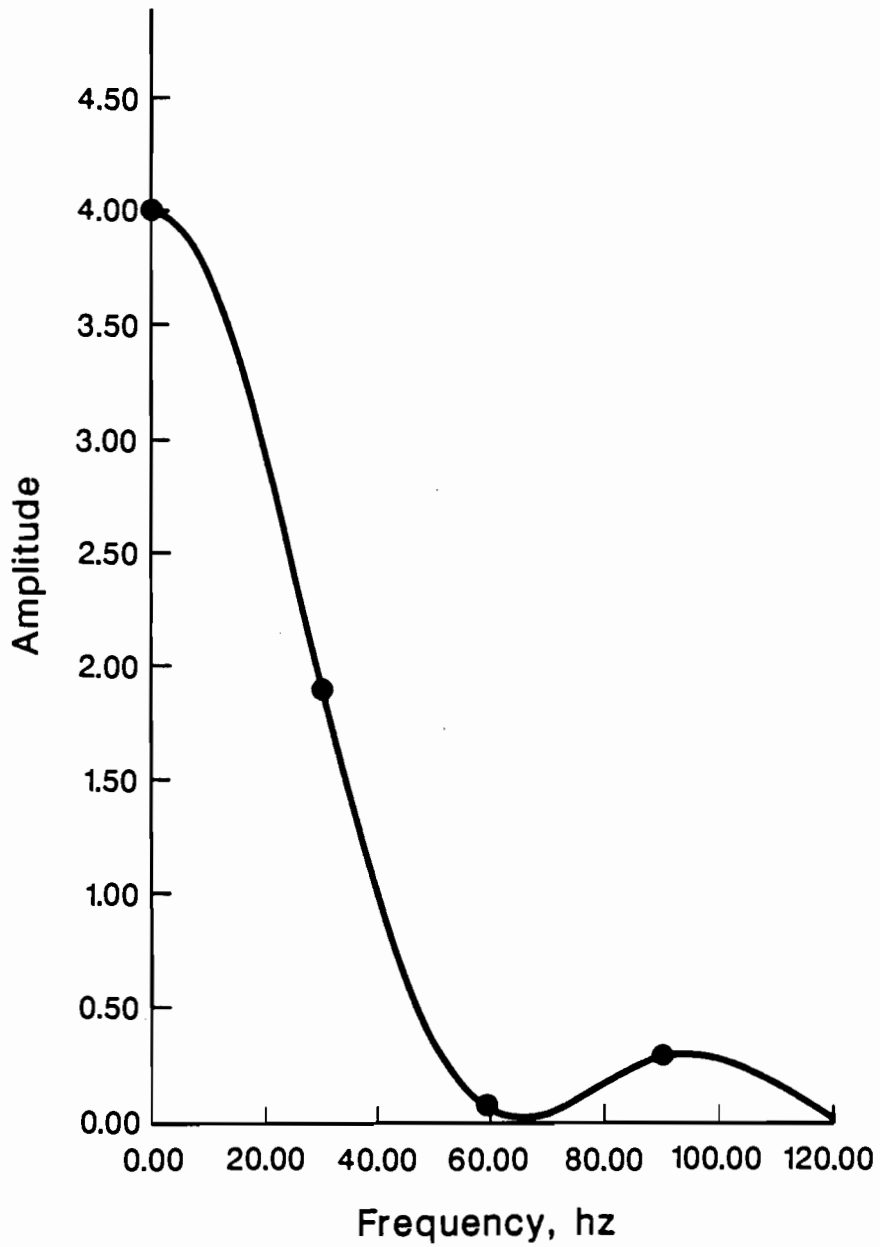


Fig. 4.3. Amplitude Spectrum of Linear Impulse Load.

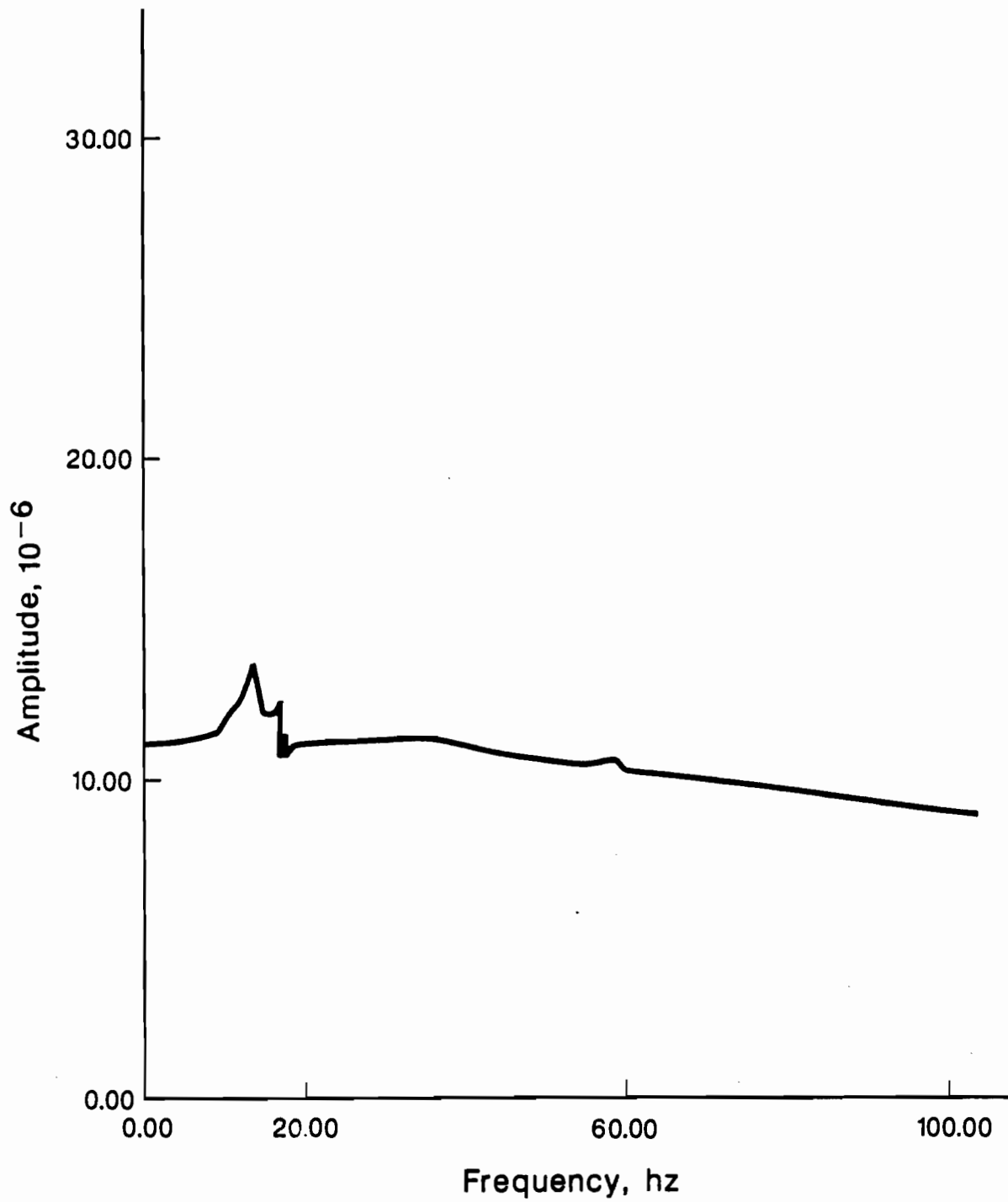


Fig. 4.4. Transfer Function at Point 1 (Center of Load) H = 20 ft - Falling Weight Deflectometer.

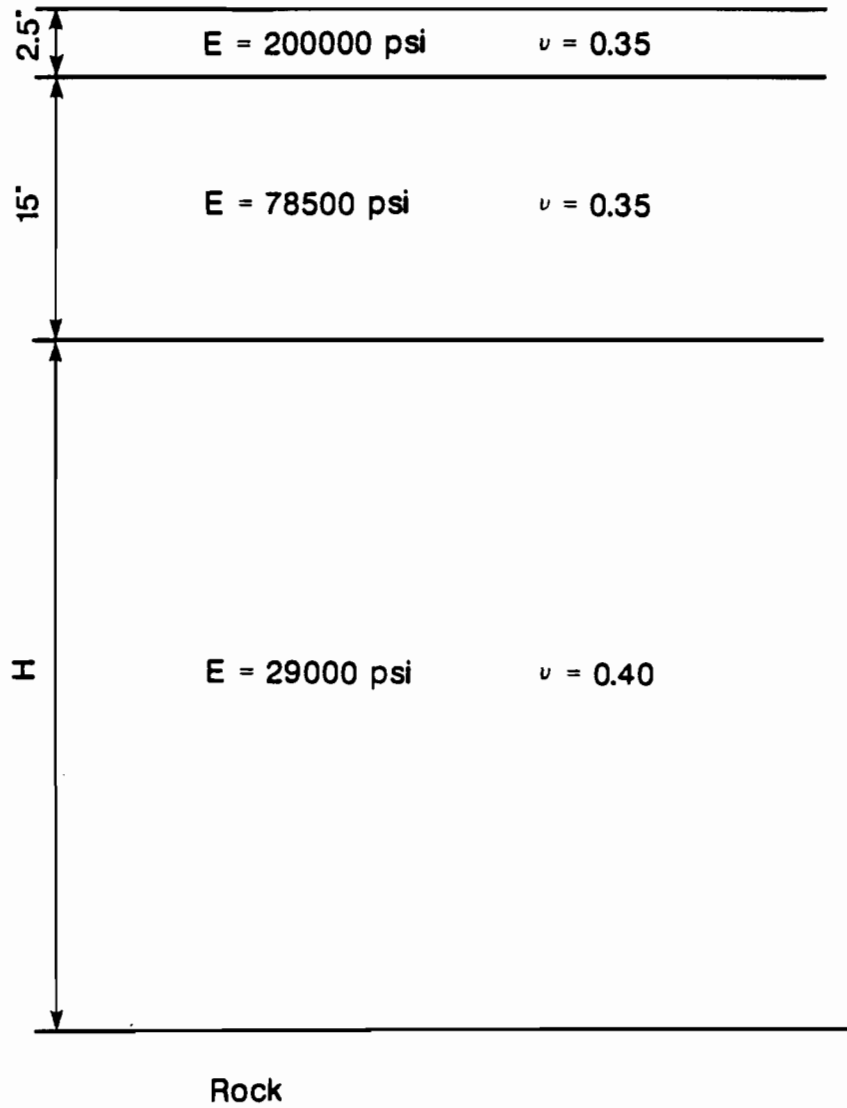


Fig. 4.5. Profile of Pavement Used for Studies.

time histories of the deflections at the various points. The complete analysis is clearly much more expensive than for the case of the Dynaflect where only one frequency is involved. Therefore the studies were limited to depths to bedrock of 10, 20, 40 and 80 feet.

The continuous Fourier transform involves an integral over time (direct transform) or frequency (inverse transform) extending from minus infinity or zero to infinity. In practice, however, a discrete transform, referred to as the Fast Fourier Transform, is used. In this case a finite number of points (power of 2) is selected to reproduce the function of time at equal time intervals Δt . The total duration is $T = N\Delta t$ if N is the number of points. Notice that for an impulse type load the values of the function will only be nonzero for a few points. The Fourier Transform is then calculated at $N/2$ points with a frequency interval $\Delta f = 1/T$ and a maximum frequency $f_{\max} = 1/2 \Delta t$. A proper selection of these parameters is important to guarantee the accuracy of the final results. A small time interval Δt is desirable to reproduce properly the time variation of the forcing function and to ensure that the peak response displacement is not missed. The total duration T should be several times larger than the actual duration of the load to ensure that spurious free vibration terms have attenuated; the appropriate value depends on the fundamental period of the system and the amount of damping (in the present case no internal damping is assumed for the soil and the only source of energy dissipation results from radiation or geometric spreading of the waves above the fundamental frequency of the soil stratum). The frequency increment Δf (fixed once the duration T has been selected) should be small to reproduce properly the transfer function, particularly if it exhibits some sharp peaks (typical of lightly damped systems). All these considerations point out the desirability of a small Δt and a large number of points N . It should be noticed, however, that as the number of points increases so does the cost of computation and the number of frequencies for which analyses must be conducted. As Δt decreases the maximum frequency f_{\max} increases, requiring more refined meshes and a larger number of layers because of the dynamic limitation on the thickness of the layers.

A number of preliminary studies were conducted to assess the required values of Δt and N to obtain reasonably accurate results. It was concluded from these studies that a value of N equal to 2048 and a time interval of approximately 0.002 seconds were appropriate for these applications. Figure 4.4 shows a typical transfer function for the center of the loaded area and a depth to bedrock of 20 feet. (The transfer function is actually complex; the amplitude

of the function is shown). It can be seen that for frequencies larger than 20 Hz the function is relatively smooth without any pronounced peaks. It was decided therefore to calculate the values of the transfer functions at frequency intervals of approximately 0.25 Hz in the range 0 to 20 Hz, 2 Hz from 20 to 60 Hz and 4 Hz from 60 to 120 Hz. Since the Δf required is of the order of 0.25 Hz the values of the transfer functions at intermediate points are evaluated by interpolation between the computed values. Finally since f_{\max} should be approximately 240 Hz the values between 120 and 240 Hz were obtained by extrapolation. The preliminary studies indicated that the results obtained with these simplifications (leading to considerable savings in computer time) were in very good agreement with those obtained using a constant frequency increment of 0.25 Hz over the complete range of frequencies.

Figure 4.6 shows typical time histories of the displacements at points 1 (center of the loaded area) and point 7 (farthest station) for a depth to bedrock of 20 feet. From these figures the peak deflection was computed at each station and the deflection bulb was obtained.

Figure 4.7 shows the static and dynamic displacement bowls for a depth to bedrock of 20 ft while Figure 4.8 shows the ratio of the dynamic to the static displacements for the same soil profile and to the static displacements assuming that the subgrade extends to infinity (the normal assumption in the interpretation of the results). It is important to notice that, once again, this ratio varies with distance to the load, increasing in general as this distance increases. The dynamic deflections are almost equal to the static ones at the center of the loaded area but become larger for the farthest stations. The ratios of the dynamic deflections to the static ones assuming a half-space are, however, close to 1, indicating that the errors committed by neglecting dynamic effects and the existence of bedrock at a finite depth tend to cancel in this case.

Figures 4.9 to 4.12 show similar results for a depth to bedrock of 40 ft and Figures 4.13 to 4.16 for a depth of 80 feet.

4.3 Estimation of Material Properties

As in the Dynaflect studies the profile of Figs. 3.1 and 4.5 was again considered with depth to bedrock in this case of 10, 20, 40 and 80 ft. Dynamic analyses were then conducted to determine the maximum displacements under an impact load simulating the force exerted by the Falling Weight

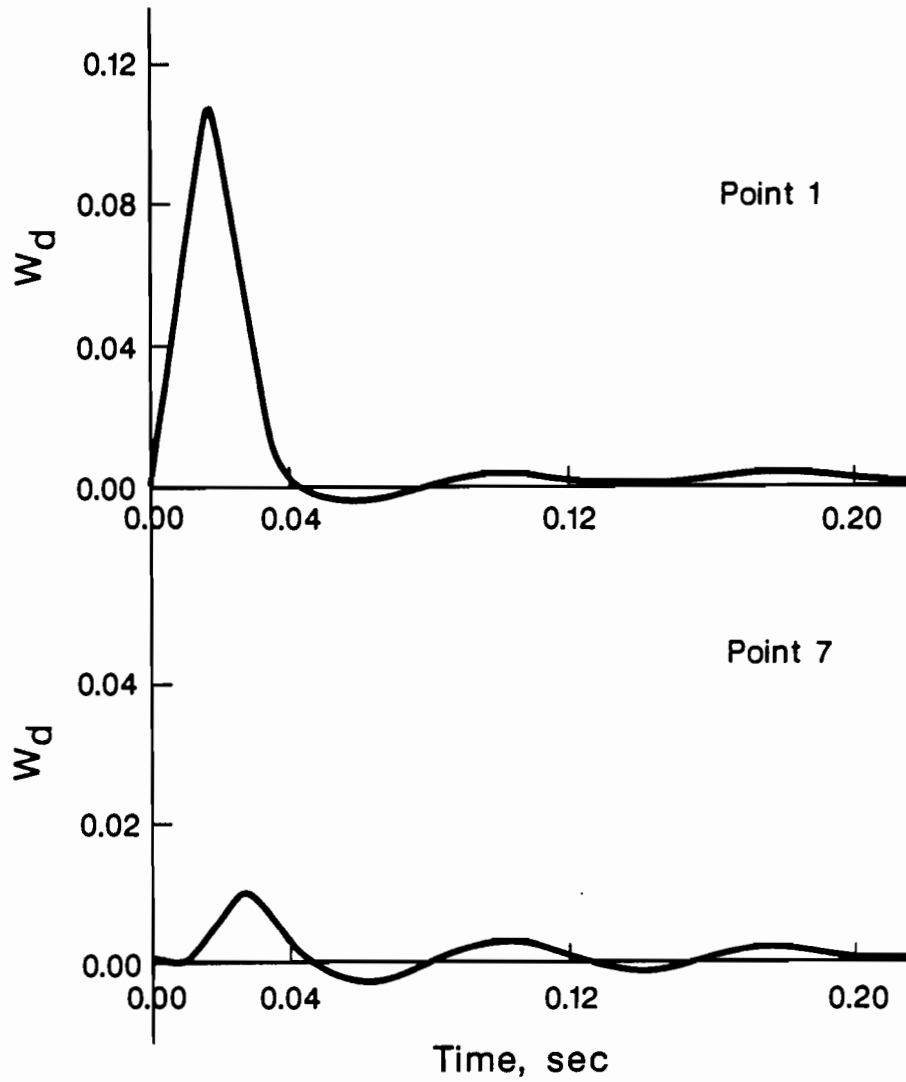


Fig. 4.6. Time History of Displacements at Points 1 and 7, $H = 20$ ft.

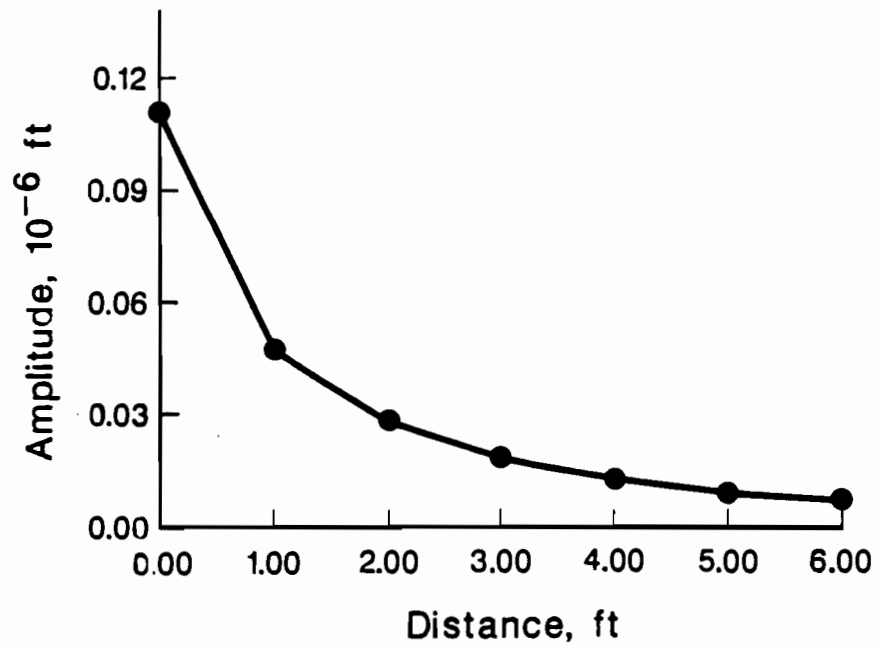
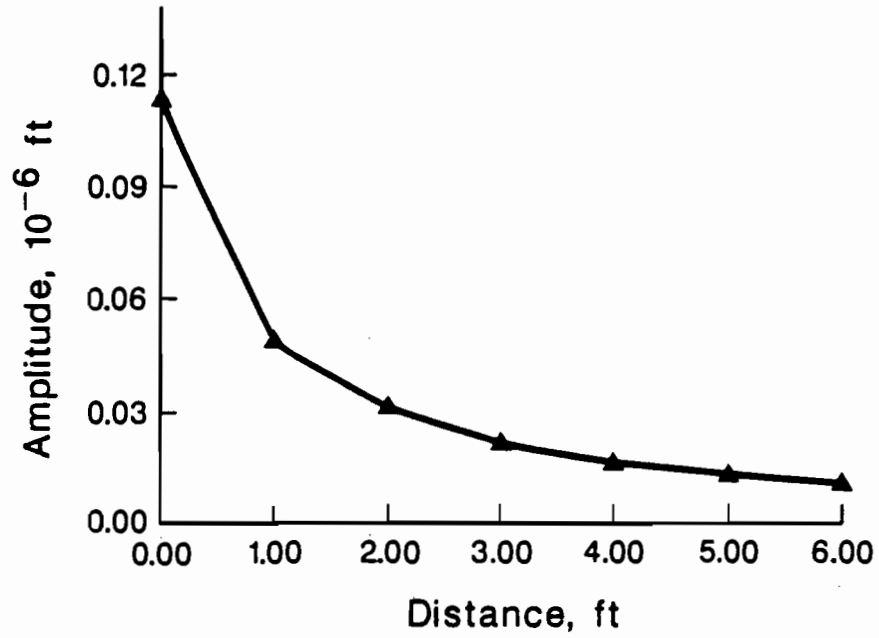


Fig. 4.7. Displacement Bowls of 1. Static, 2. Dynamic, $H = 20$ ft.

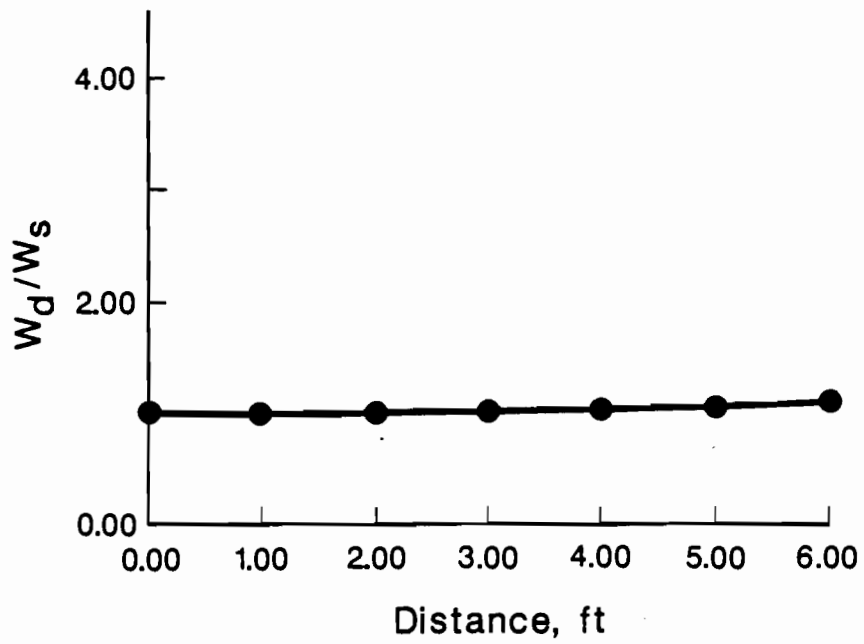
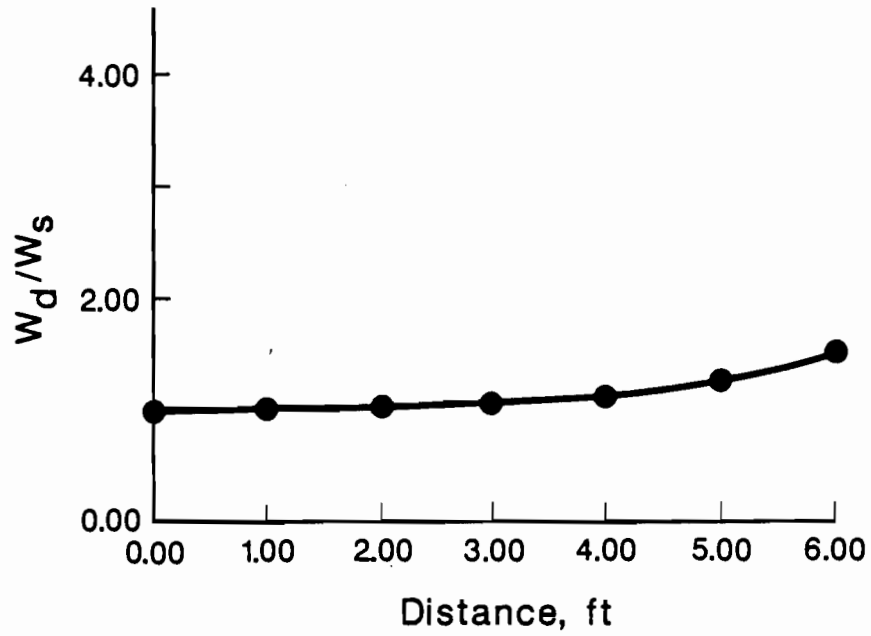


Fig. 4.8. Ratio of Dynamic (Imp.) to Static and Static ($H = \infty$) Displacements, $H = 20$ ft - Falling Weight Deflectometer.

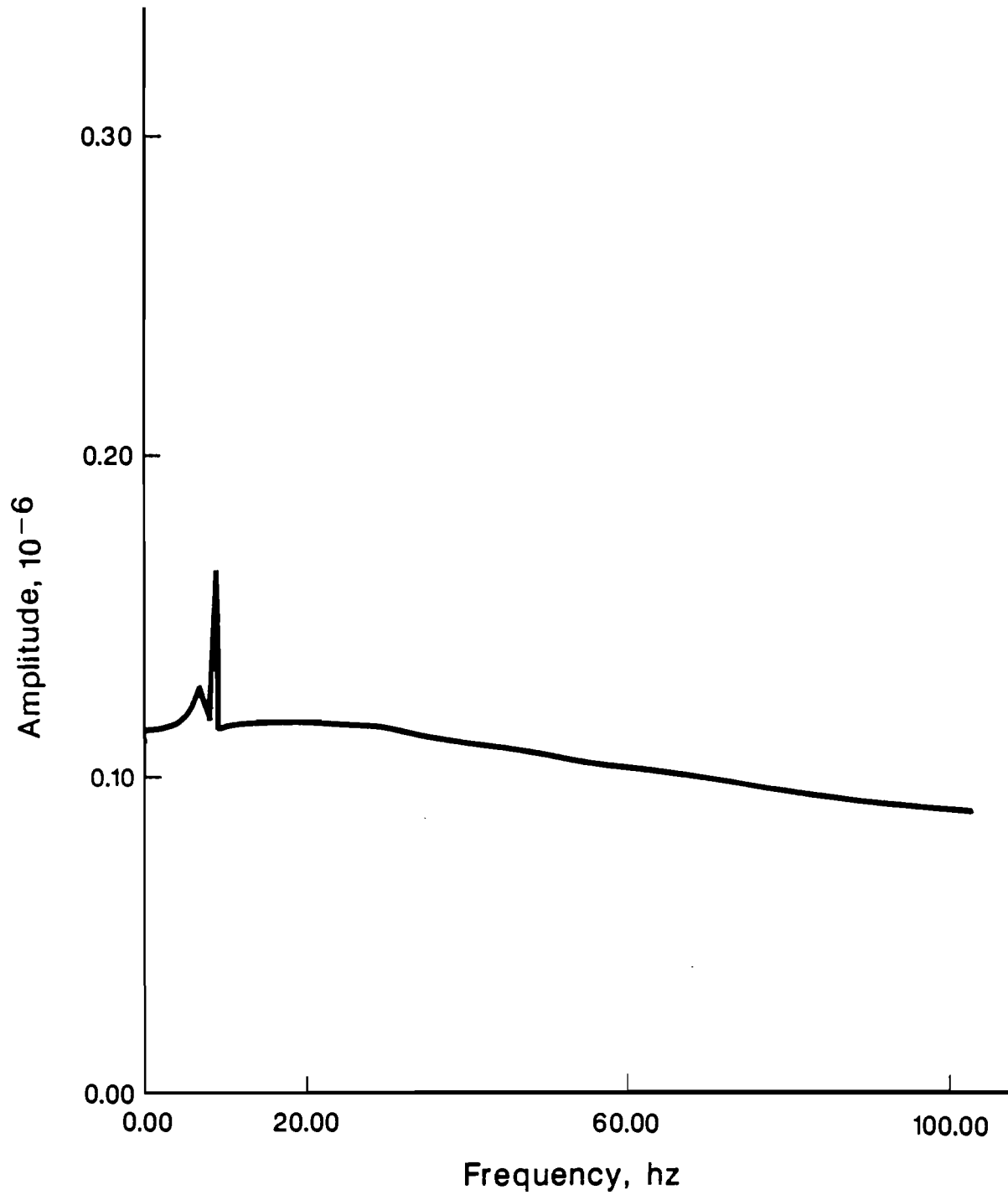


Fig. 4.9. Transfer Function at Point 1 (Center of Load), H = 40 ft - Falling Weight Deflectometer.

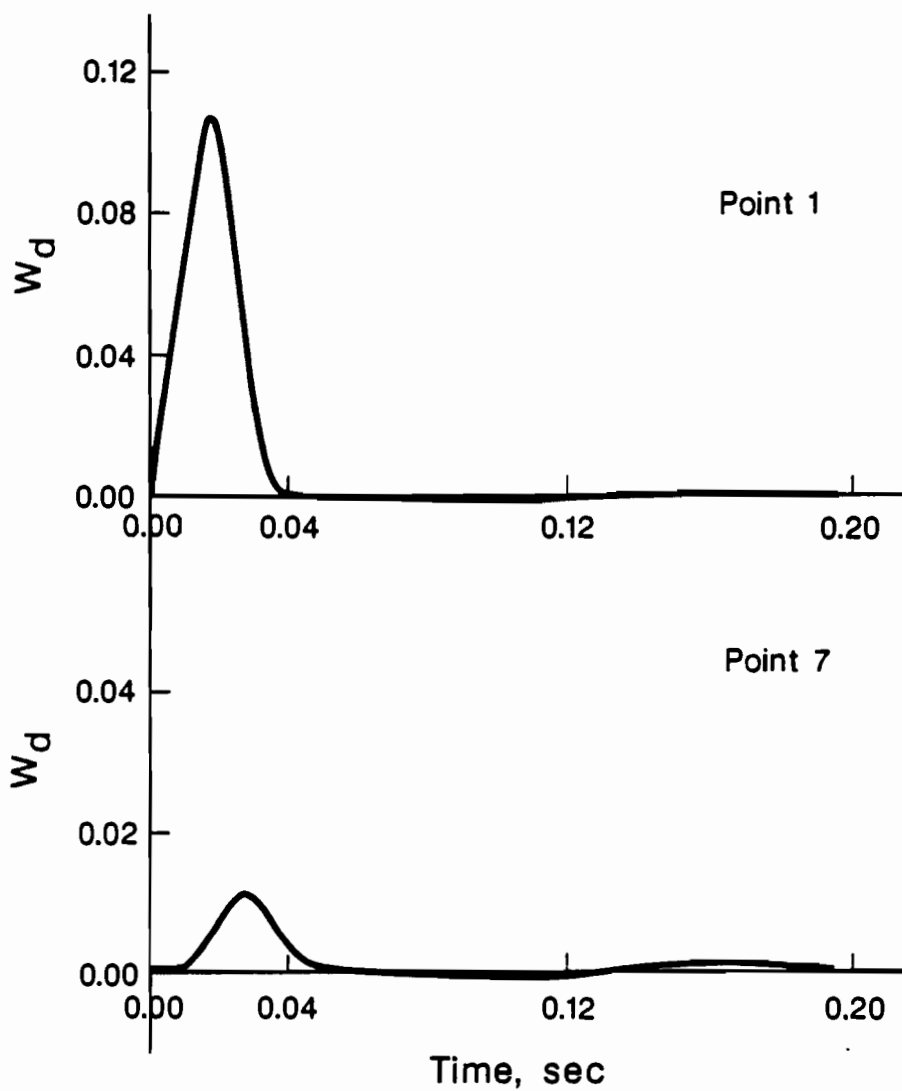


Fig. 4.10. Response Time History of Displacements at Points 1 and 7, $H = 40$ ft - Falling Weight Deflectometer.

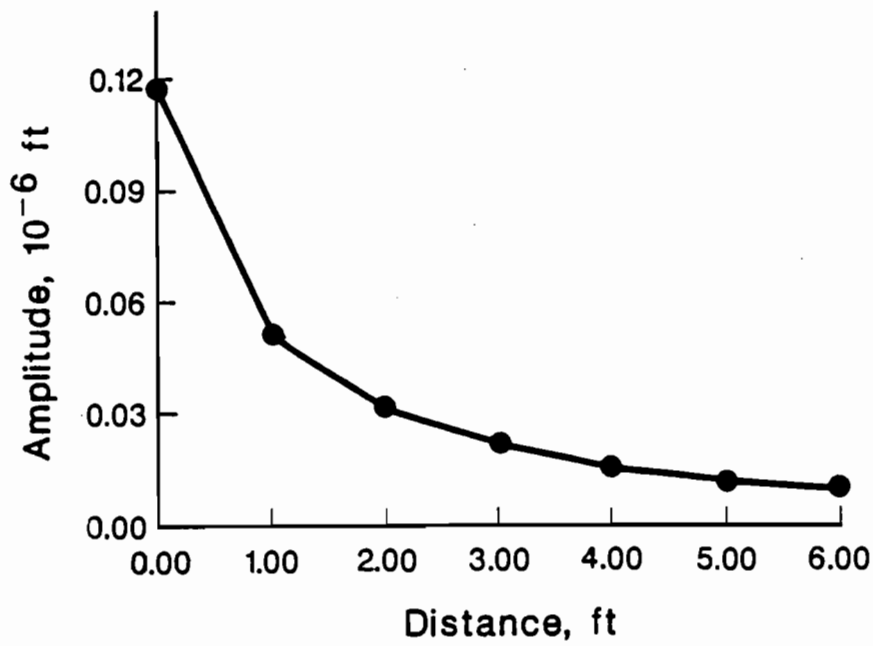
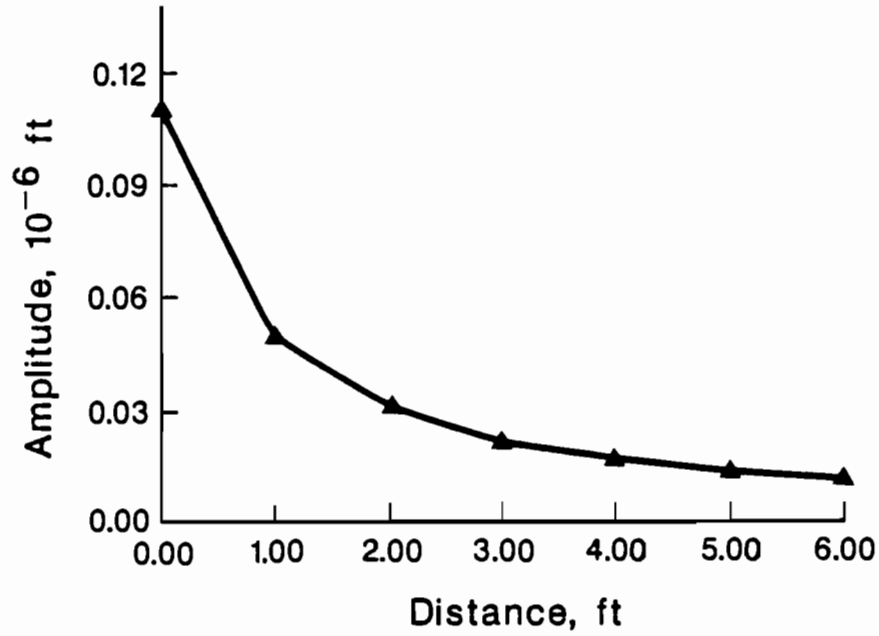


Fig. 4.11. Displacement Bowls of 1. Static, 2. Dynamic, $H = 40$ ft.

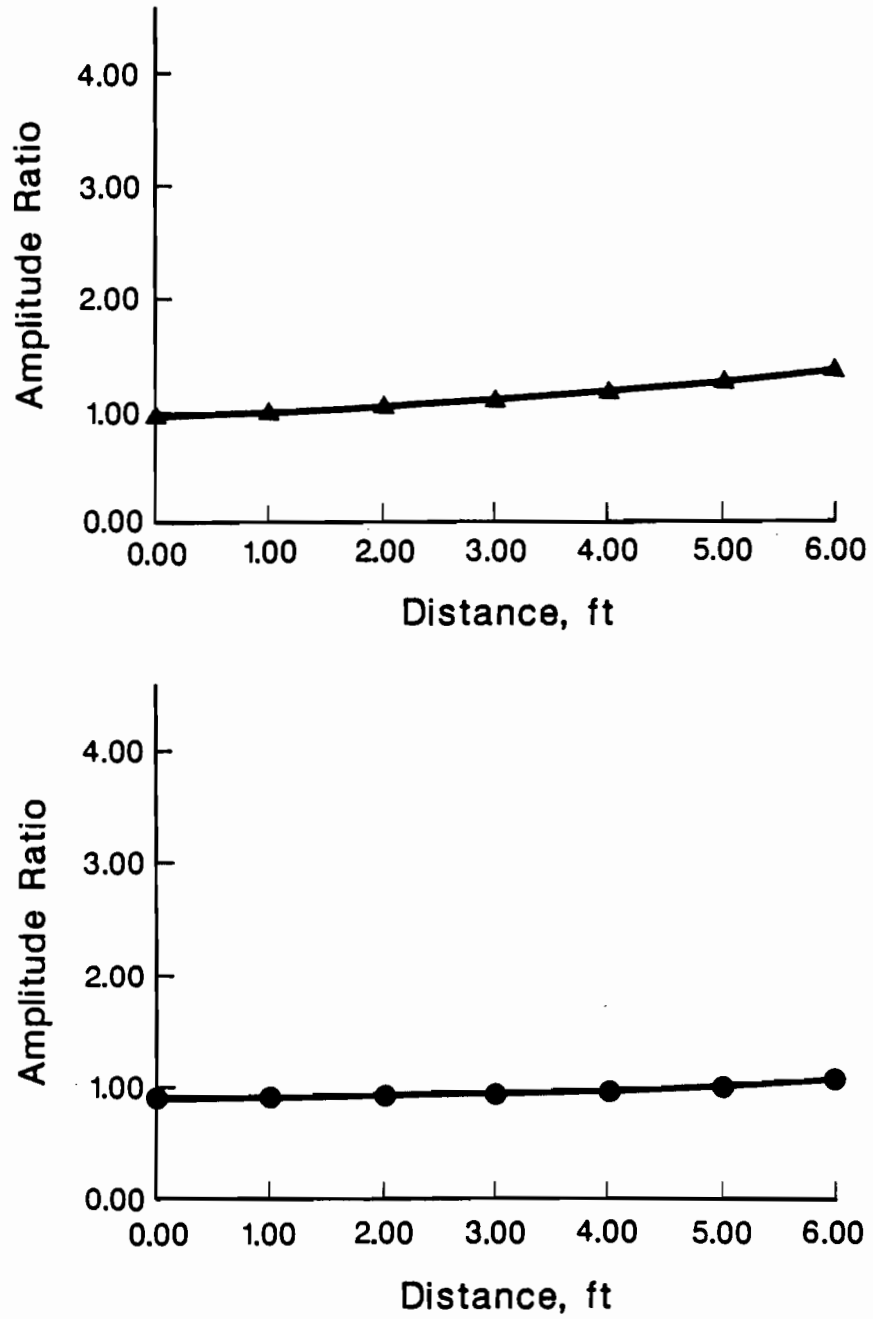


Fig. 4.12. Ratio of Dynamic to Static and Static ($H = \infty$) Displacements, $H = 40$ ft - Falling Weight Deflectometer.

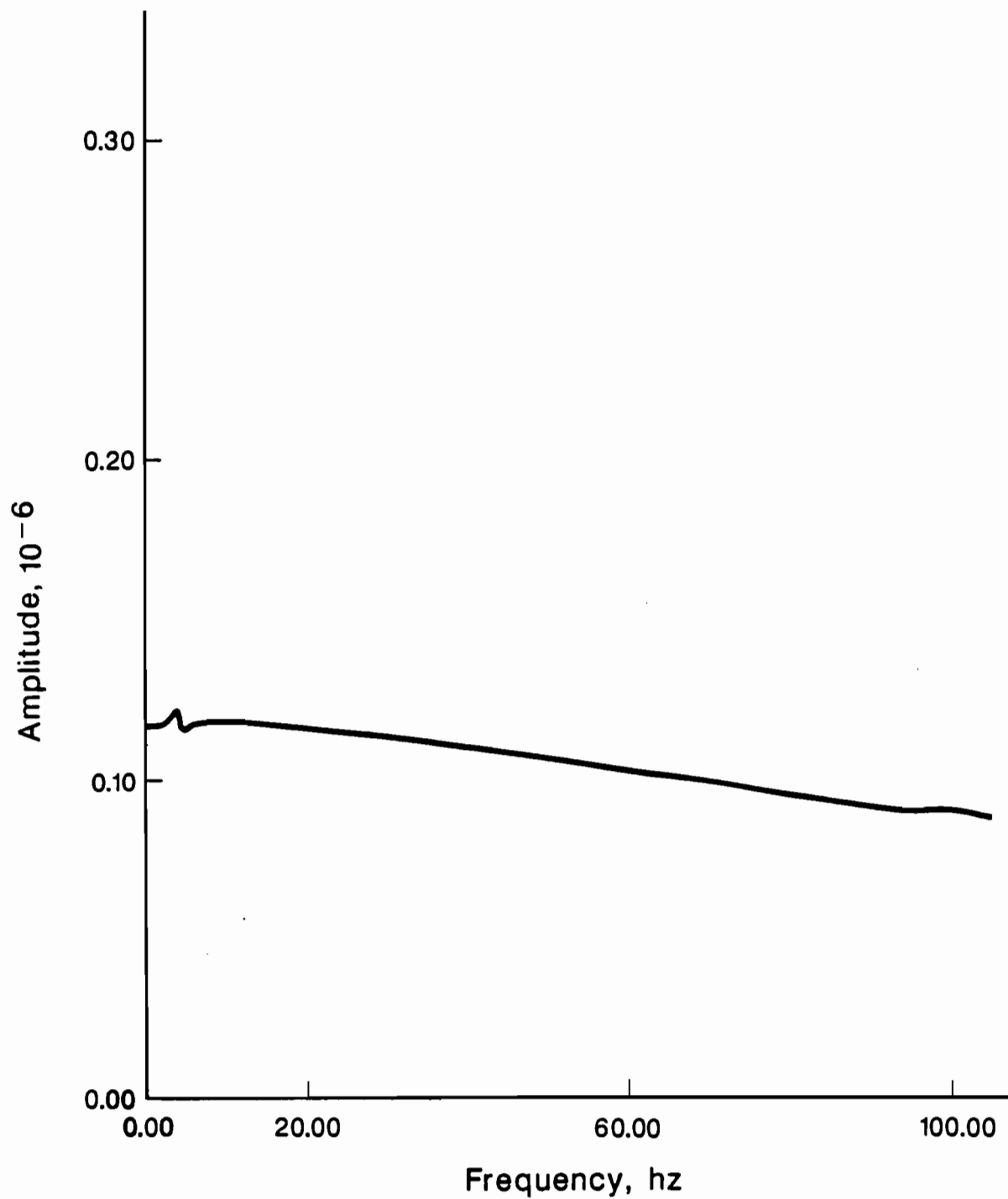


Fig. 4.13. Transfer Function at Point 1 (Center of Load), H = 80 ft - Falling Weight Deflectometer.

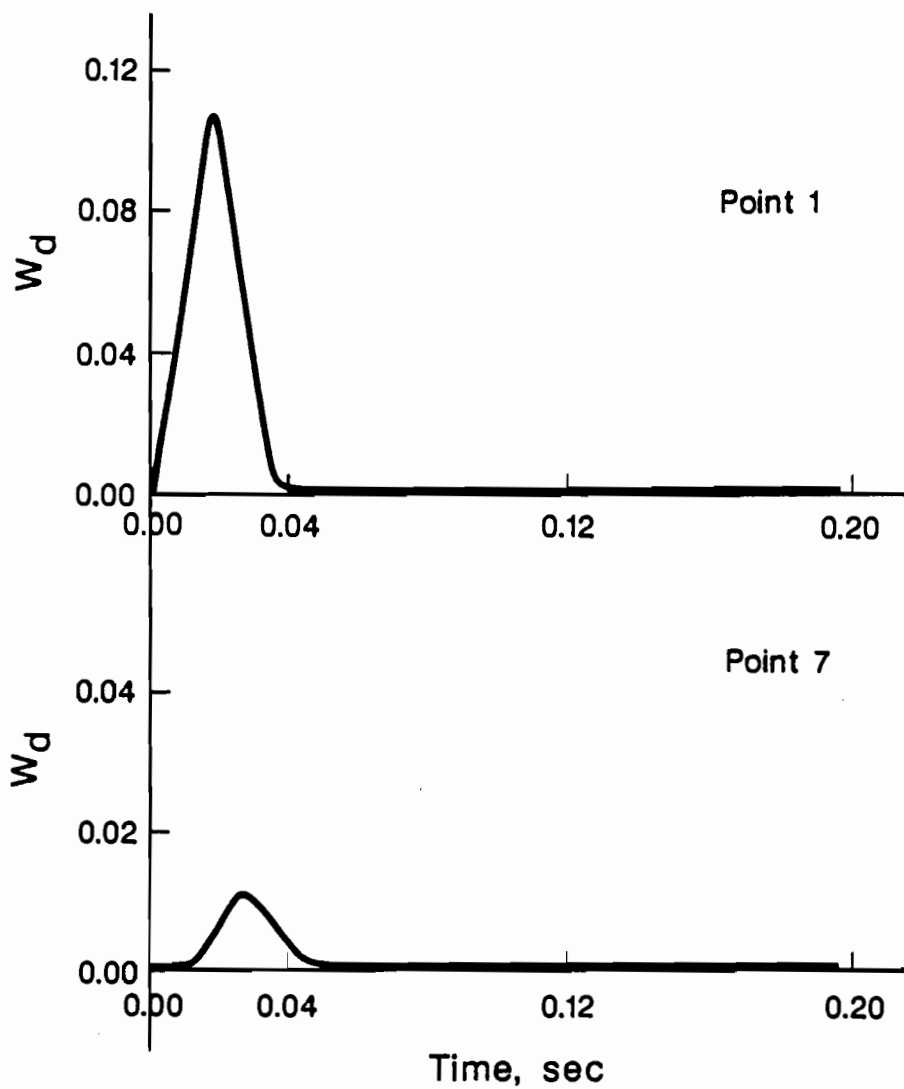


Fig. 4.14. Response Time History of Displacements at Points 1 and 7, $H = 80$ ft, Falling Weight Deflectometer.

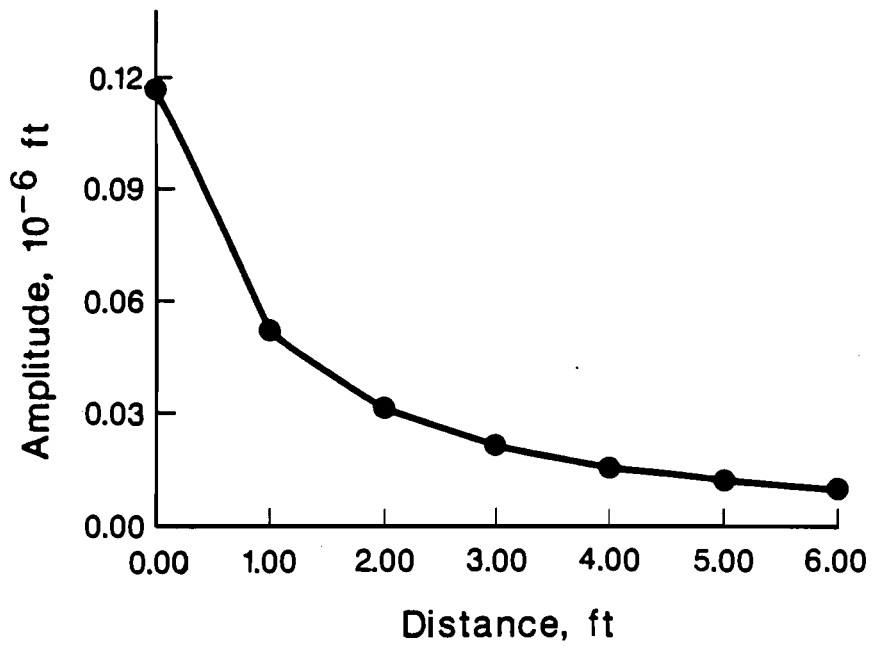
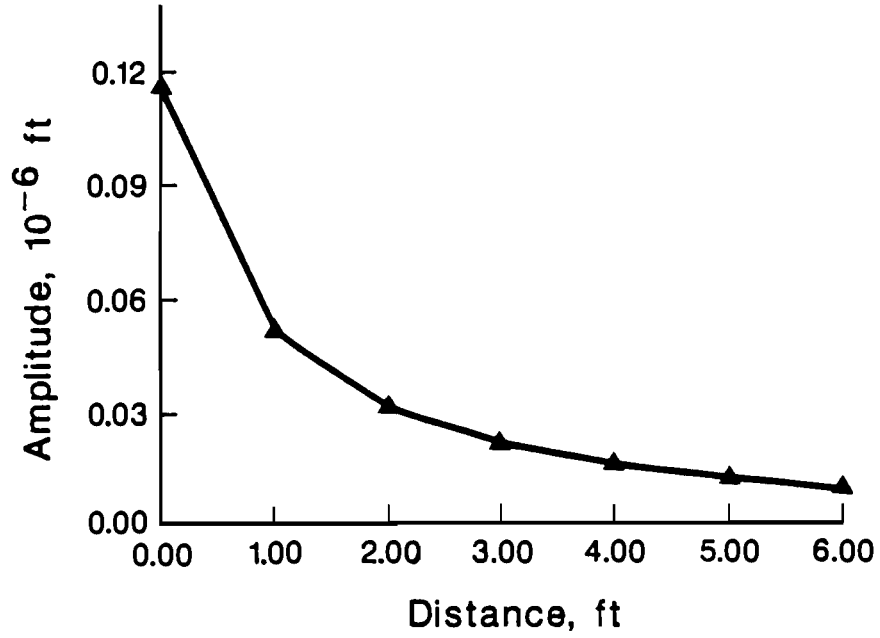


Fig. 4.15. Displacement Bowls of 1. Static, 2. Dynamic, $H = 80$ ft.

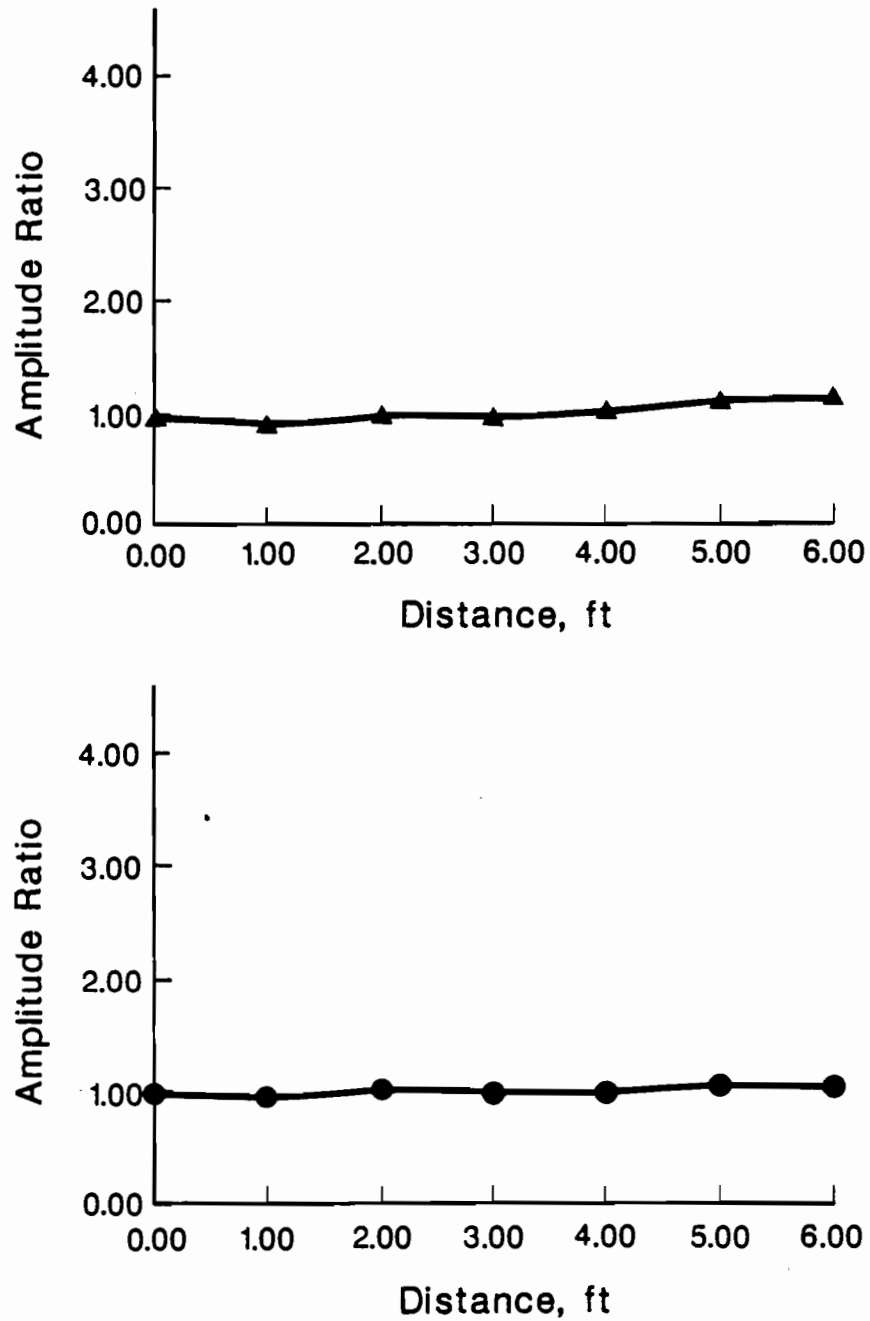


Fig. 4.16. Ratio of Dynamic to Static and Static ($H = \infty$) Displacements, $H = 80$ ft - Falling Weight Deflectometer.

Deflectometer, at the seven stations used typically with this instrument. The dynamic displacements were then used as input to backfigure elastic moduli using iterative static analyses. The procedure used for this simulation was identical to that described in Section 3.3 the only difference being in the load used for the dynamic analyses. It must be emphasized again that uniqueness of the solution is not guaranteed with this approach and that a different set of moduli might provide results within the same tolerance. The problem is inherent in the procedure used at present to backfigure the elastic properties of the pavement system.

The results of these analyses are shown in Table 4.1. The static displacements assuming that the subgrade extends to infinity and the dynamic displacements for depths to bedrock of 10, 20, 40 and 80 ft are tabulated together with the actual and predicted elastic properties and the errors involved in the estimates. For this pavement system the errors are always much smaller than those reported in Table 3.1 for the Dynaflect tests. Even so, it should be noticed that the small differences between static and dynamic deflections can introduce errors in the estimates (particularly for a depth to bedrock of 40 ft) due to the distortion in the shape of the displacement bowl (the fact that the ratio of dynamic to static displacements is slightly less than 1 under the load and slightly larger at the farthest stations).

Due to the cost of computation it was not possible to repeat these studies for the case where the soil properties in the subgrade increase with depth instead of remaining uniform, a situation of practical significance. Additional studies should be conducted before the conclusions from this example can be generalized. It appears, however, that dynamic effects are less important for the Falling Weight Deflectometer than for the Dynaflect due to the fact that a broader range of frequencies is involved instead of a single frequency.

TABLE 4.1. DEFLECTION BULBS AND PREDICTED ELASTIC MODULI FOR HOMOGENEOUS SUB-BASE AND DIFFERENT DEPTHS TO BEDROCK. FALLING WEIGHT DEFLECTOMETER.

Displ. ($\times 10^{-8}$ ft)		Distance to the Center							Young's Modulus (lb/in ²)	Errors (%)
		0'	1'	2'	3'	4'	5'	6'		
Static	H=inf.								200,000	
		11.54	5.139	3.141	2.180	1.611	1.253	1.015	78,500	
										29,000
Dyn.	H=10ft								200,000	0.0
		10.60	4.622	2.842	1.923	1.317	0.9094	0.7214	78,500	0.0
										35,539
Dyn.	H=20ft								200,000	0.0
		11.06	4.652	3.013	2.073	1.538	1.280	1.090	82,200	4.7
										28,790
Dyn.	H=40ft								287,200	43.6
		10.74	4.860	3.008	2.111	1.590	1.288	1.086	87,375	11.3
										28,331
Dyn.	H=80ft								200,000	0.0
		11.08	4.733	3.073	2.109	1.608	1.311	1.044	89,131	13.5
										29,245

CHAPTER 5. CONCLUSIONS AND RECOMMENDATIONS

The main objective of this work was to develop a more accurate model to compute the displacements at points along the surface of a pavement due to a dynamic excitation, either at a fixed frequency or in the form of an impact. A discrete formulation was selected because it is particularly efficient when dealing with a large number of horizontal layers with different properties, as would be encountered in practice if the modulus of the subgrade increased with depth. When dealing on other hand with an elastic half-space or a very small number of layers the formulation presented by Apsel (3) would be more convenient.

The formulation was implemented in a computer program and a number of parametric studies were conducted to assess the accuracy of the results as a function of the number and thickness of the layers, and the distance from the point of application of the load (or the center of the loaded area) to the point where displacements are computed. The results of these studies indicated that the deflections near the load are affected only by the properties of the material near the surface while the properties at depth play an increasing role as the distance to the load increases. A procedure to select an appropriate mesh for a given distance and frequency of vibration was derived on the basis of these preliminary studies and used for all ensuing analyses.

The computer program developed was used then to assess the importance of dynamic effects on the results of typical Dynaflect and Falling Weight Deflectometer tests when the soil in the subgrade is underlain at a finite depth by much stiffer rock. An actual pavement system was selected for these studies varying the depth to bedrock (thickness of the subgrade). For this particular profile the results indicate that a static interpretation of the displacement bowl measured in Dynaflect tests might be reasonable when dealing with a homogeneous soil (subgrade) extending to depths of 40 ft or more. When much stiffer bedrock is encountered at shallower depths important dynamic amplifications can occur and the elastic properties backfigured for the pavement system using standard techniques can be substantially in error. The situation is aggravated when the soil in the subgrade is not homogeneous but its stiffness increases with depth. For the profile studied dynamic effects were then important up to

a depth of 60 feet. In general dynamic effects due to the existence of bedrock at a finite depth will be significant if the frequency of excitation (typically 8 Hz for the Dynaflect) is in the range between the fundamental frequencies of the profile in shear and dilatation. It is recommended that these frequencies be estimated in cases where the results seem unusual.

Dynamic effects seem to be less important for the Falling Weight Deflectometer, where a broad range of frequencies are excited rather than a single one. For the particular case studied the errors introduced by neglecting dynamic effects and the existence of bedrock at a finite depth tended to cancel each other resulting in dynamic displacements for the actual profile very similar to the static deflections assuming a half-space for the subgrade. Even so there were still some ranges of depth to bedrock for which the difference in dynamic effects at the various stations, distorting the shape of the displacement bowl, leads to erroneous estimates of the elastic moduli. Due to the cost of computation it was not possible to study the case where the properties of the soil in the subgrade increase with depth. Additional studies are recommended to generalize the conclusions related to the Falling Weight Deflectometer.

An additional problem with the Dynaflect and the Falling Weight Deflectometer is that only a small set of values (five or seven deflections) is available to backfigure the elastic properties of the pavement, base and subgrade. A procedure which takes advantage of much more information is the Spectral Analysis of Surface Waves.

BIBLIOGRAPHY

1. Achenbach, J.D., Wave Propagation in Elastic Solids, North Holland Publishing Co., Amsterdam, 1973.
2. Aki, Keiti, "Scattering and Attenuation," BSSA, Vol. 72, No. 6, pp. 2319-s330, December 1982.
3. Apsel, R.J., "Dynamic Green's Functions for Layered Media and Applications to Boundary Value Problems," Doctoral Thesis - University of California, San Diego, 1979.
4. Brebbia, C.A., The Boundary Element Method for Engineers, John Wiley & Sons, New York, 1978.
5. Eagleson, Bary, Scott Heisey, W. Ronald Hudson, Alvin H. Mayer, and Kenneth H. Stokoe, II, "Comparison of the Falling Weight Deflectometer and the Dynaflect for Pavement Evaluation," Research Report 256-1, Center for Transportation Research, The University of Texas at Austin, November 1982.
6. Ewing, W.M., W.S. Jordetsky, and F. Press, Elastic Waves in Layered Soil and Foundations, Prentice-Hall, Englewood Cliffs, New Jersey, 1970.
7. Gazetas, G., "Dynamic Stiffness Functions of Strip and Rectangular Footings on Layered Soils," S.M. Thesis, M.I.T., Civil Engineering Department, 1975.
8. Haskel, N.A., "The Dispersion of Surface Waves on Multilayered Media," BSSA, 43, No. 1, February 1953.
9. Heisey, J. Scott, Kenneth H. Stokoe, II, W. Ronald Hudson, and A.H. Meyer, "Determination of In Situ Shear Wave Velocities from Spectral Analysis of Surface Waves," Research Report 256-2, Center for Transportation Research, The University of Texas at Austin, November 1982.
10. Johnson, L.R., "Green's Function for Lamb's Problem," Journal of Geophysics, Vol. 37, pp. 99-131, 1974.
11. Karabalis, D.L., and D.E. Beskos, "Dynamic Response of 3-D Rigid Surface Foundations by Time Domain Boundary Element Method," Earthquake Engineering and Structure Dynamics, Vol. 12, pp. 73-93, 1984.
12. Kausel, E., "Forced Vibrations of Circular Foundations on Layered Media," Research Report R74-11, Department of Civil Engineering, M.I.T., 1974.
13. Kausel, E., "An Explicit Solution for the Green Functions for Dynamic Loads in Layered Media," Research Report S81-13, M.I.T., 1981.
14. Kausel, E., and J.M. Roesset, "Stiffness Matrices for Layered Soils," BSSA 71, No. 6, December 1981.

15. Kennett, B.L.N., "Seismic Waves in a Stratified Half-Space-ii. Theoretical Seismograms," Journal of Geophysics, Vol. 61, pp. 1-10, 1980.
16. Lysmer, John, "Lumped Mass Method for Rayleigh Waves," Bulletin of the Seismological Society of America, Vol. 60, pp. 89-104, February 1970.
17. Nazarian, S., and K.H. Stokoe, II, "Evaluation of Modulus and Thickness of Pavement Systems by SASW Method," Research Report 256-4, Center for Transportation Research, The University of Texas at Austin, 1983.
18. Nazarian, Soheil, K.H. Stokoe, II, W.R. Hudson, "Use of Spectral-Analysis-of-Surface-Waves Method for Determination of Moduli and Thickness of Pavement System," a paper presented at the Annual Meeting of the Transportation Research Board, January 1983.
19. Nazarian, Soheil, and K.H. Stokoe, II, "Nondestructive Testing of Pavements Using Surface Waves," a paper presented at the Annual Meeting of the Transportation Research Board, January 1984.
20. Schlue, J.W., "Finite Element Matrices for Seismic Surface Waves in Three-Dimensional Structures," BSSA, Vol. 69, No. 5, pp. 1425-1237, October 1979.
21. Spain, Barry, and M.G. Smith, Functions of Mathematical Physics, Van Nostrand Reinhold Company, London, 1970.
22. Tassoulas, J.L., "Elements of the Numerical Analysis of Wave Motion in Layered Media," M.I.T., Research Report R 81-2, Order No. 689, Department of Civil Engineering, M.I.T., Cambridge, Mass., February 1981.
23. Thomson, W.T., "Transmission of Elastic Waves through a Stratified Soil Medium," Journal of Applied Physics, 21, February 1950.
24. Uddin, Waheed, Soheil Nazarian, W. Ronald Hudson, Alvin H. Meyer, and Kenneth H. Stokoe, II, "Investigations into Dynaflect Deflections in Relation to Location/Temperature Parameters and Insitu Material Characterization of Rigid Pavements," Research Report 256-5, Center for Transportation Research, The University of Texas at Austin, December 1983.
25. Waas, G., "Linear Two-Dimensional Analysis of Soil Dynamics Problems on Semi-Infinite Layered Media," Ph.D. Thesis, University of California, 1972.
26. Wang, C.Y. and R.B. Herrmann, "A Numerical Study of P, SV and SH-Wave Generation in a Plane Layered Medium," BSSA, pp. 1015-1036, August 1980.